Techno-economic analysis of CCUS in Sweden

Fanney Einarsdóttir, Seonggyun Kim, Maja Larsson, Erik Readwin, Rosa Sandén, Alexander Singh, Sanna Védrine, Martin Wood

Supervisors: Dr. Michael Greencorn and Dr. Shareq Mohd Nazir

December 13^{th} 2024

Abstract

This report studies the techno-economic feasibility of implementing Carbon Capture, Utilization, and Storage (CCUS) technologies in Sweden. focusing mainly on two critical industries, cement and pulp. This was done by studying two production plants: the Slite Cement Plant and the Korsnäs Pulp Plant. The chosen plants were due to one mainly being a source of biogenic CO_2 from Korsnäs and the other mainly fossil in nature from Slite. The key objective is to reduce CO_2 emissions while aligning with the Sustainable Development Goals (SDGs). AspenPlus v14 was used to simulate and design the CO_2 capture and utilization system used in the project. Using 30 wt % monoethanolamine (MEA)-based absorption for high efficiency and scalability. The captured CO_2 was assessed in two downstream processes: permanent storage with Northern Lights and the chemical utilization for methanol synthesis.

The economic evaluation considers capital and operational expenditures (CapEx and OpEx) for each pathway, incorporating site-specific flue gas compositions, process design optimizations, and sensitivity analyses. The results show that carbon utilization is a potential source of revenue, but at a higher cost, and eventually, emissions are offset by CO_2. In contrast, CO storage$_2$ has robust climate benefits by removing greenhouse gasses from the atmosphere but lacks financial benefits for biogenic carbon emissions. For fossil-based CO_2, carbon credits were found as a source of income. Key performance indicators (KPIs) such as cost per captured carbon (CCC), net present value (NPV), and return on investment (ROI) highlight the trade-offs between environmental impact, cost-effectiveness, and scalability. The report concludes with the future of carbon capture and what needs to change for it to be sustainable from an economic standpoint.

Foreword

We would like to express our gratitude to our supervisor, Dr. Michael Greencorn, whose feedback, support, and guidance were crucial throughout this project. His expertise and encouragement gave us the confidence to navigate challenges and aim for success.

We would also like to thank Professor Shareq Mohd Nazir for his support and readiness to assist us whenever needed.

Finally, the rest of the group would like to thank our amazing team leader, Sanna Védrine. Her excellent organization and ability to keep everything under control made her an outstanding leader throughout this project.

List of Tables

List of Figures

Contents

1 Introduction

1.1 Background

Carbon dioxide (CO_2) is a greenhouse gas that accumulates in the atmosphere and contributes significantly to global warming. One way of decreasing the amount of CO_2 that is emitted is replacing fossil fuels with renewable energy sources, which do not increase the amount of CO_2 in the atmosphere over time. While it is urgent to transition to renewable energy sources instead of burning fossil fuels, certain critical industries face challenges in completely removing their CO_2 emissions. For example, the construction sector relies on the production of cement which produces CO_2 as a by-product. The pulp industry also releases CO_2, which in that case is biogenic due to the processing of biological material [1, 2]. Therefore, Carbon Capture Utilization and Storage (CCUS) technologies that can be retrofitted to the effluent streams of existing chemical plant facilities have the potential to decrease the negative environmental impact of these industries while continuing to operate. After the carbon is captured, it can then either be stored (Carbon Capture Storage, CCS) or used as a raw material in other applications such as for the production of methanol (Carbon Capture Utilization, CCU), see Figure 1.

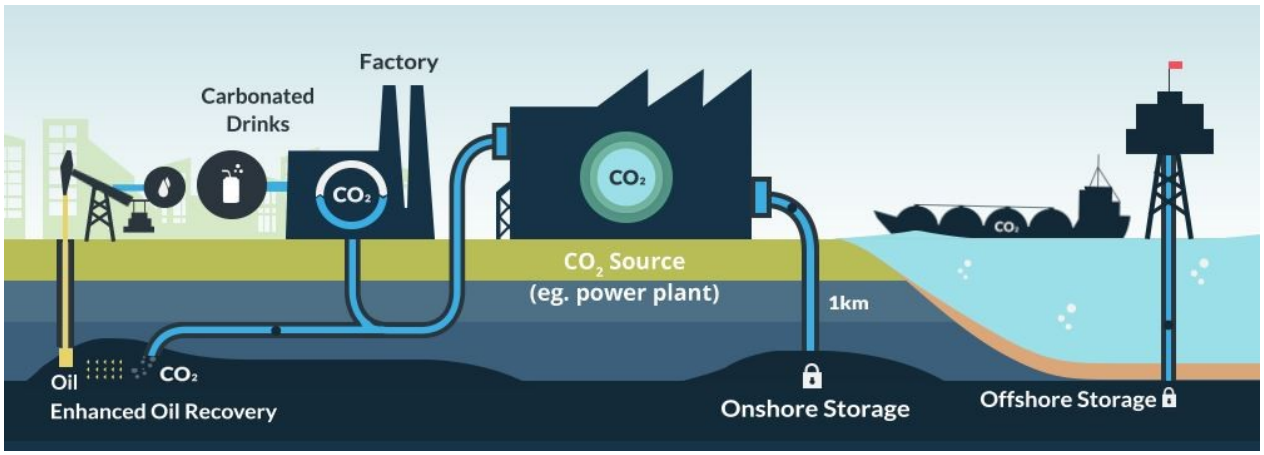

Figure 1: An overview of Carbon Capture Utilization and Storage [3].

In CCS, the captured carbon is transported to an underground storage site, which can be onshore or offshore [4]. The transport is most often through pipelines or ships. The reservoir containing the stored CO_2 can be of different sorts, for example, a depleted gas or oil field or a deep saline aquifer. For CCU, the captured carbon can be revalorized for other purposes. It can be used directly, for example, bound in construction products or alternatively, it can be used as a feedstock and be converted into chemical products such as methanol, oil, or plastics.

1.2 Sustainable Development Goals

The Sustainable Development Goals (SDGs) are the United Nations framework for addressing climate change and mitigating its negative effects. Since CCS and CCU are both technologies

to implement sustainability industrially, they naturally align with some of the SDGs. Table 1 shows the SDGs that have a direct and indirect interaction with the effects of CCS and CCU. Having a direct interaction means that the CCUS itself affects the SDG in some way, while indirect interactions are when the CCUS has for example upstream or downstream effects on the SDG [5, 6].

Table 1: SDGs with Direct and Indirect Interaction with CCS and CCU.

SDG Category	**Direct Interaction**	**Indirect Interaction**
Environmental	SDG 13	SDG 14
Social	SDG 7	SDG 11
Economic	SDG 9, SDG 12	N/A

Environmental SDGs are the goals that impact the environment. SDG 13 addresses taking urgent action to combat climate change and its impacts. Both CCS and CCU contribute positively to this goal by capturing the CO_2 that would be emitted to the atmosphere, and instead storing it in safe deposits or converted into methanol to be used again. Thus, the greenhouse effect is counteracted, especially with CCS. SDG 14 is about conserving and sustainably using the oceans, seas, and marine resources for sustainable development. This is not entirely related to carbon capture, but rather indirectly. Since CCS is about reducing the amount of carbon emitted, there will be less interaction between carbon and masses of water and hence a lower contribution to ocean acidity.

Economical SDGs are the SGDs with financial aims. SDG 9 has direct interactions with CCS and CCU which is about building resilient infrastructure, promoting inclusive and sustainable industrialization, and fostering innovation. Both CCS and CCU are innovative solutions that promote sustainable industrialization, so they align well with SDG 9. SDG 12 is to ensure sustainable consumption and production patterns. Clearly, CCS ensures sustainable consumption by burying the emission products, and CCU ensures sustainable production patterns by transforming carbon from emissions to new fuels, instead of using fossil resources.

Social SDGs affect the wellbeing and welfare of people. SDG 7 aims to ensure access to affordable, reliable, sustainable, and modern energy for all. This aligns well since CCU is the definition of modern energy. However, how reliable and affordable it is depends on what energy source is used to produce the methanol from the CO_2. SDG 11, to make cities and human settlements inclusive, safe, resilient, and sustainable, applies indirectly, since CCS and CCU overall create a more sustainable environment, but the plants could also disturb the areas where they operate.

1.3 Formulation of Problem

The first step to reduce CO_2 emissions in industrial processes is to assess the feasibility of retrofitting existing facilities with CCUS technologies. This requires analyzing the technical and economical aspects of carbon capture, utilization, and storage processes.

1.3.1 Aim and Objectives

The aim of the project is to find the most economically suitable way of addressing carbon emissions from two main points: a cement plant in Slite, Gotland, and a pulp factory in Korsnäs. The primary objective of this investigation is the recommendation of the downstream application for the captured CO_2 based on a techno-economic analysis.

Firstly, the Carbon Capture Utilization and Storage (CCUS) processes for different effluent types and downstream applications (storage or utilization) will be designed based on literature data on carbon storage, capture, and utilization technologies and processes. The different kinds of scenarios possible will be further discussed in Section 1.3.3. Secondly, the economic study will analyze the capital and operating expenditures, and revenue, and perform a sensitivity analysis. This will in turn be used to calculate the following key performance indicators (KPIs); Cost per captured carbon (CCC), net present value (NPV), and return on investment (ROI). These metrics can then be used to compare the economic feasibility of each alternative.

1.3.2 Delimitations

The delimitations of this project include the main CCU and CCS processes. The processes will be retrofitted to the effluent of industrial plants and the feed for the CO_2 capture will be limited to data based on existing cement and pulp facilities. The only utilization application for the captured CO_2 will be direct hydrogenation for methanol production, though other applications exist but will not be considered within the scope of this investigation. The hydrogen (H_2) for the direct hydrogenation step will not be produced on-site and will be sourced from a H_2 production plant. Additionally, all electricity used in the process will be from renewable sources. The delimitations are summarized in Figure 2 below.

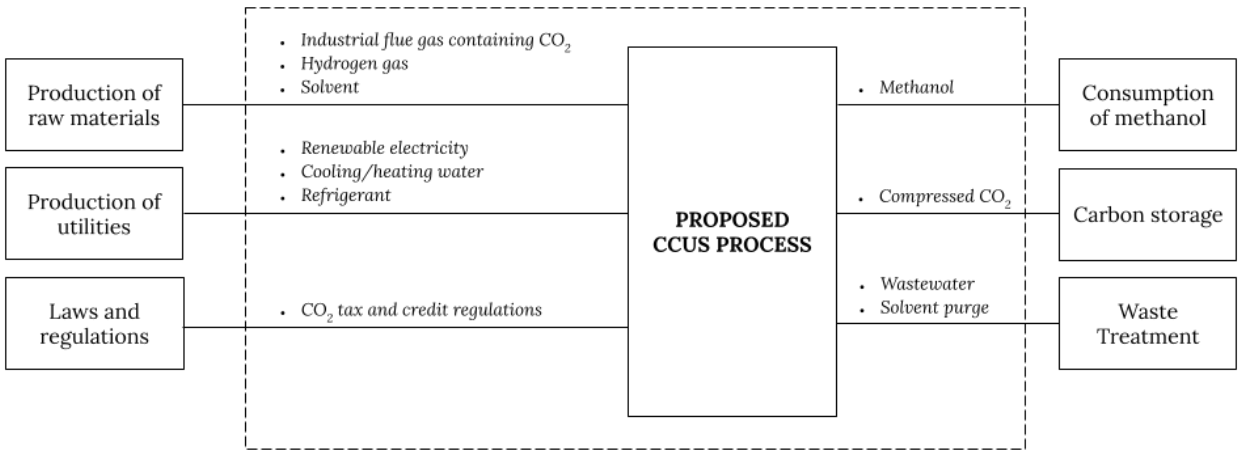

Figure 2: Delimitations for CCUS techno-economic analysis.

1.3.3 Scenarios for Consideration

Since the project scope considers two types of emissions, from cement and pulp plants, as well as two downstream applications for the captured carbon, utilization and storage, there are four possible scenarios to consider as summarized in Table 2 below.

The main differences that are considered with the emissions from cement and pulp plants are the molar compositions and the overall flow rates. These factors will affect the size and energy consumption and eventually the cost of the project. Additionally, the type of carbon emission, biogenic or fossil, will affect the potential revenue based on the carbon credit or tax regulations as discussed later.

The motivation for carbon utilization is that there are financial incentives in selling the methanol produces in the process. However, the carbon will still be emitted and will still ultimately contribute to the greenhouse effect. The motivation for carbon storage is that the carbon would not reach the atmosphere at all since the carbon is permanently encapsulated and cannot contribute to the greenhouse effect. In fact, if the CO_2 that is captured comes from biogenic sources, it results in negative emissions.

Table 2: Different scenarios for CO_2 usage.

Case No.	**Feed Type**	**Carbon Application**
1	Cement	Utilization
2	Cement	Storage
3	Pulp	Utilization
4	Pulp	Storage

2 Industrial Plants for CCUS Retrofitting

Retrofitting industrial facilities with CCUS technologies require evaluating, emission types, processing capacity, and site planning to ensure the necessary infrastructure.

2.1 Emission Classifications

There are two types of CO_2 emissions as shown in Figure 3: fossil and biogenic. Fossil emissions come directly from finite, fossil fuels while biogenic emissions come from natural, renewable sources. Capturing fossil CO_2 emissions decreases the overall pollution and greenhouse effect approaching a net-zero effect whereas capturing biogenic CO_2 contributes to negative emissions, since these emissions are not considered to contribute to the greenhouse effect due to their renewable nature.

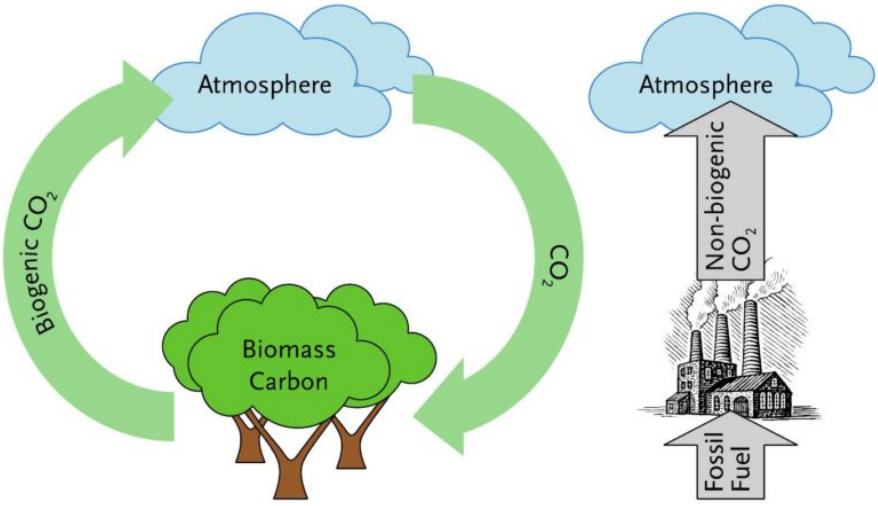

Figure 3: Biogenic carbon cycle vs fossil emissions [7].

2.2 Industrial Plant Carbon Emissions

The cement and pulp plants were chosen since they differ in primary type of carbon emission. The pulp plant mainly consumes renewable materials which results in biogenic emissions whereas the cement plant emissions produces mostly fossil emissions from incineration of finite materials and fuels.

2.2.1 Slite Cement Plant

The cement plant that will be used as a model in this project is the Slite plant in Gotland, Sweden. A simple overview of the whole process from mining to distribution is shown in Figure 4 below.

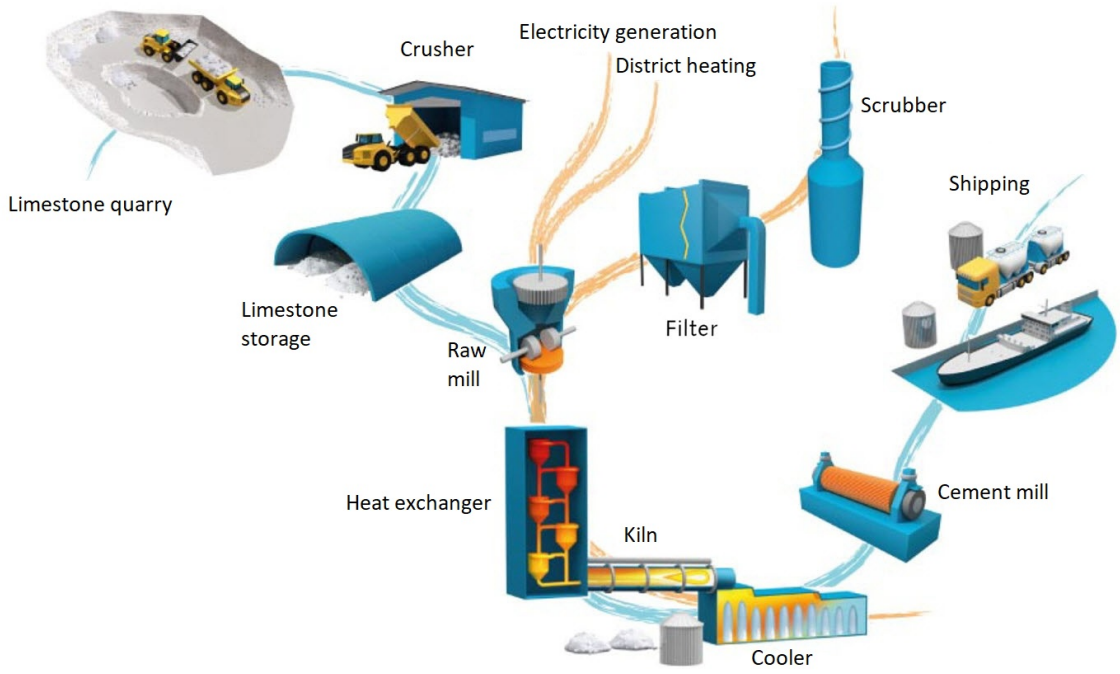

Figure 4: Process diagram of Slite cement plant [8].

In Slite, 69% of the fuel is recycled and a quarter is from biogenic sources and the rest is from fossil sources [9]. The main CO_2 emission points are from the limestone incineration and the combustion in the kiln which contribute 50% each to the total emissions [10]. Both of these points are in close proximity to each other, both connected to the kiln, so they are assumed to be combined into one stream. The carbon emissions from limestone incineration are classified as fossil emissions since limestone is a finite material. However, the CO_2 from the fuel combustion is partly biogenic because of the mixture fuel. According to data from Naturvårdsverket, the biogenic part of the total stream of CO_2 is about 13% [11].

Table 3: Generic composition of cement plant flue gases [12].

Species	Composition (mol%)
O_2	7.5
H_2O	18.2
CO_2	17.8
N_2	56.5

From the same source, there were compositions of CO, SO_2 and NO_x gases as well, but in much smaller quantities. Those concentrations were measured to 1 887, 14, and 237 ppm respectively, and were therefore negligible when calculating the overall flow rate.

2.2.2 Korsnäs Pulp Plant

The primary sources of CO_2 emissions from a pulp mill are the recovery boiler, bark boiler, and the limekiln. However, all streams of hot flue gas are brought together and fed into

steam turbines which become the main emission point [13]. A bark boiler is also called a power boiler. The Korsnäs pulp mill production is 97% fossil free [14]. A process diagram of the Korsnäs pulp plant is shown in Figure 5 below.

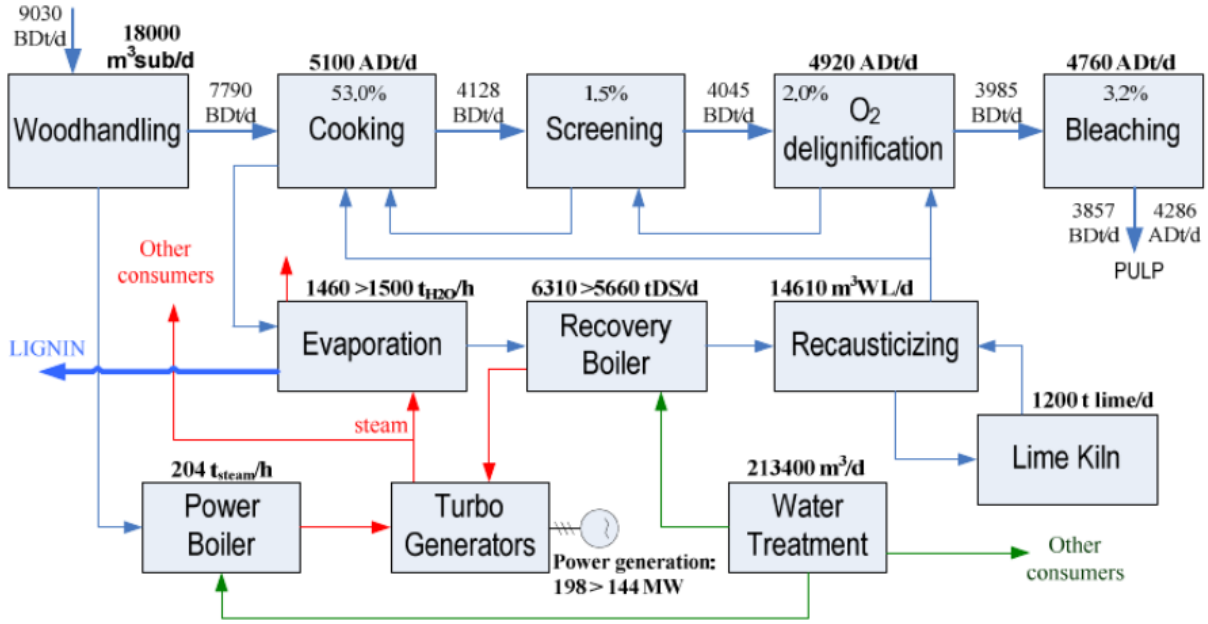

Figure 5: Process diagram of Korsnäs pulp plant [15].

The generic outlet composition for flue gas from pulp plants is summarized in Table 4 below.

Table 4: Generic composition of pulp plant flue gases.

Species	Composition (mol%)
O_2	1.2
H_2O	30.9
CO_2	20.4
N_2	47.4

As shown in Table 4, the total flow rate of the flue gas from the pulp plant is 6.22×10^5 m^3/h. Again, the substances in smaller amounts were not included in the volumetric flow rate. The SO_x and NO_x concentrations were both very small, 50 and 175 ppm respectively.

2.2.3 Summary

Table 5 summarizes the background information, plant capacity and emissions for both the cement and pulp plants selected for this feasibility study. As displayed in Table 5, the total flow rate out of the Slite cement plant is about 8.03×10^5 m^3/hour and for the pulp plant about 6.22×10^5 m^3/hour. This was estimated from the general composition of cement and

pulp plant flue gases shown in Table 3 and 4 respectively by calculating all the flow rates from the molar compositions there together with the emission data in Table 5 and adding them up to a total flow.

Table 5: General information about cement and pulp plants [11, 16].

	Cement plant	**Pulp plant**
Information		
Name	Slitefabriken, Heidelberg Materials Cement AB	Korsnäsverket, Billerud
Location	Slite, Gotland, Sweden	Gävle, Sweden
Plant Capacity		
Product	2.5×10^6 t-cement/year	7.5×10^5 t-cardboard/year
Flue gas	8.03×10^5 m^3/hour	6.22×10^5 m^3/hour
CO_2 emissions		
Fossil CO_2	1 337 734 t-CO_2/year	16 377 t-CO_2/year
Biogenic CO_2	174 237 t-CO_2/year	1 128 694 t-CO_2/year

2.3 Site planning

To effectively plan for building the carbon capture, carbon storage, and carbon utilization processes, a suitable location for the facilities needs to be determined. This includes determining whether or not there is enough space on the chosen industrial facilities onsite or if the process or parts of the process will need to be relocated offsite. Since there are challenges finding the correct correlation between plant production and physical size, the methodology used for determining the right areas for the plants is outlined below:

1. An existing plant with the required capacity is chosen and its area measured using Google Earth.
2. A place with the measured amount of area is searched for in the proximity of the cement and pulp plants.
3. It can be decided if the process can be implemented onsite or if the CO_2 has to be moved offsite.

2.3.1 Carbon capture plants

Firstly, carbon capture plants need to be built for the cement and the pulp production. In Slite, there are already plans to build a carbon capture and storage plant [17]. The place chosen for the plant is *Östra Brottet*, which is 20 ha (200 000 m^2), and can capture, compress and temporarily store 1.8 million t-CO_2/year. A model of the future CCS plant at Slite is shown from two angles in Figure 6.

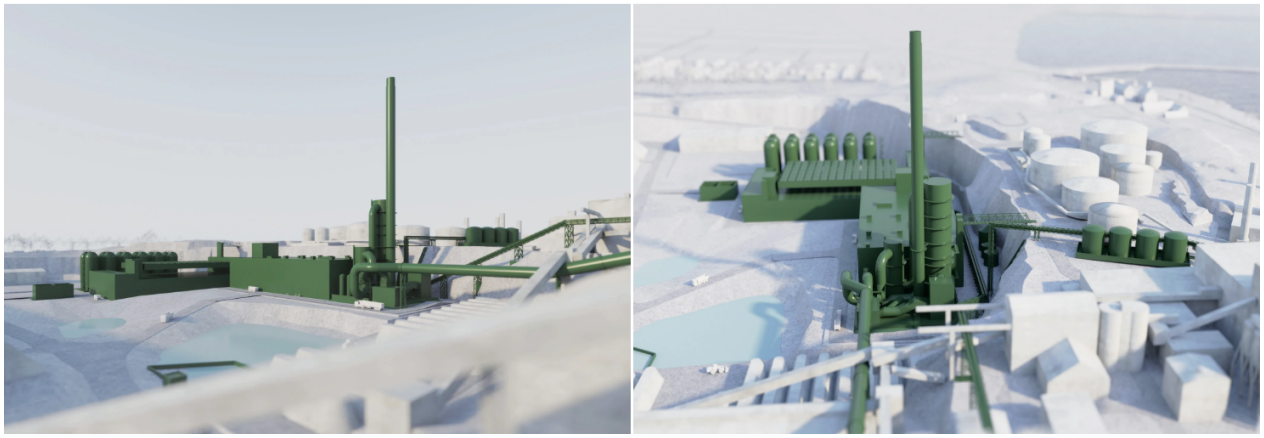

Figure 6: A model of the future carbon capture plant in Slite [18].

Since a place already is found for the carbon capture in Slite, now a place with the same dimensions at Korsnäsverket needs to be found. The capacity of the Slite CCS plant is also enough for the carbon capture from the pulp plant, which produces 1.5 Mt-CO_2/year compared to the cement plant's 1.8 Mt-CO_2/year (see Table 5) which means that 20 ha will be enough for this plant as well. An unused part south-east of the pulp plant was measured to about 33 ha and therefore chosen as the carbon capture site for pulp production. Figure 7 displays the area in satellite view.

Figure 7: Site chosen for the pulp carbon capture.

2.3.2 Methanol plants

After having captured the carbon, it needs to be converted into methanol if one of the carbon utilization scenarios are chosen. To be able to conduct the utilization onsite, there has to be an area large enough for the methanol plant available close to respective production plant. However, firstly the size of the plant has to be decided. Here, an existing plant with the right

or slightly higher consumption of CO_2 as the production plants produces is searched for. The closest to 1.8 million t-CO_2/year, which corresponds to the cement emission, was found in the Topsoe methanol plant in Turkmenistan which consumes about 2.6 Mt-CO_2/year [19]. The site was measured to about 55 ha, which then is what will be needed for the methanol plants that are to be built.

As the size of the methanol plant is determined, the second step is to find somewhere to build it. The first choice would be onsite, and therefore the area around Slitefabriken is explored. Quite close to the site, an old quarry called *Västra brottet* stands depleted [20]. This is about 74 ha and could hence be used as site for the methanol plant in Slite. The place is marked on the map in Figure 8 below.

Figure 8: Site chosen for the Slite methanol production plant.

For the pulp methanol plant, a site near Korsnäsverket is desirable. After scouting the area and ascertaining where all the nature reserves and residential areas where, a piece of land about > 200 ha was found in close proximity to Korsnäsverket. The area is displayed in Figure 9.

Figure 9: Site chosen for the Korsnäs methanol production plant.

3 Technology Literature Review

This section presents a comprehensive technical review about carbon capture, utilization, and storage. For each of these processes within the overall CCUS framework, several options of process technologies, configurations, materials, and other factors are considered. These evaluations are then used as the foundation for designing a complete process in Section 4.

3.1 Carbon Capture

There is a wide range of carbon capture technologies with various industrial applications and levels of technological maturity. Broadly, carbon capture technology can target CO_2 at two primary points: either directly from ambient air (Direct Air Capture, DAC) or at an industrial emission point. For emission-based capture, technologies can be classified into three primary approaches based on the stage of the process at which capture occurs: pre-combustion, oxyfuel combustion, or post-combustion as shown in Figure 10 below [21].

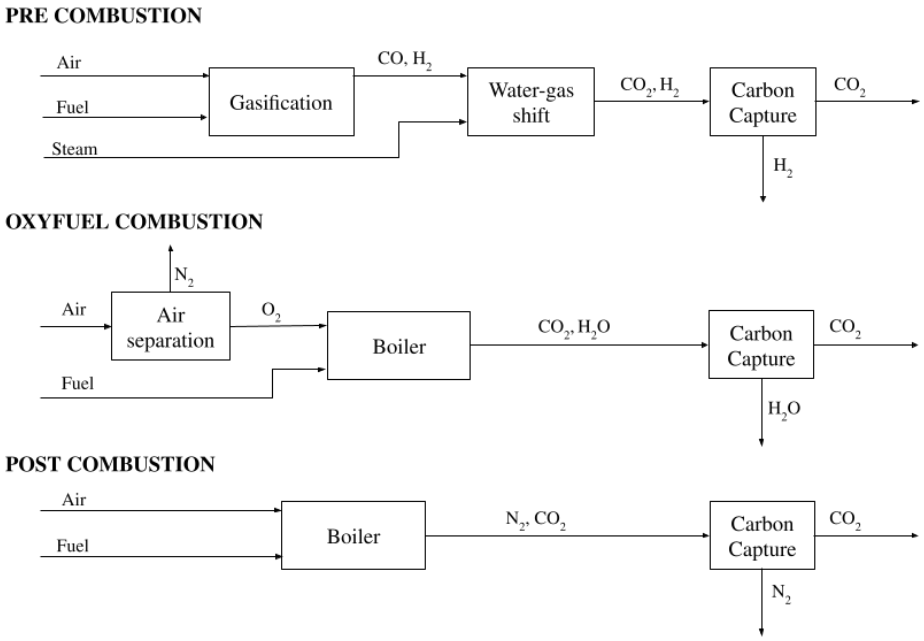

Figure 10: Carbon capture approach classifications. Based on [22].

Pre-combustion capture involves carbon-rich fuels such as coal or biomass which are gasified to produce syngas, which is a mixture of carbon monoxide (CO) and hydrogen (H_2). The CO is then converted to CO_2 in a water-gas shift reaction. This allows CO_2 to be separated early in the process and the hydrogen can be used as clean fuel. Pre-combustion is a commercially available technology and can be retrofitted but only into existing gasifying facilities [21]. One benefit is that the stream entering the carbon capture unit has a higher CO_2 concentration which means the system will have lower energy requirements. For example, to achieve 90% capture efficiency, pre-combustion capture requires about 3.35 GJ/t-CO_2 [23].

Oxyfuel combustion capture involves burning fuel in pure oxygen instead of air, producing flue gases composed of CO_2 and water vapor. The high concentration of CO_2 simplifies

the capture, as the water can easily be condensed out [21]. The main drawback is the amount of energy required to produce pure oxygen, which increases the cost and energy penalty. Additionally, high CO_2 concentrations can lead to corrosion. Oxyfuel systems can achieve over 90% capture efficiency, using around 4.05 GJ/t-CO_2[23].

Post-combustion capture involves extracting CO_2 from flue gases of traditional combustion processes using air, where CO_2 is diluted with nitrogen and other contaminants. It is the most developed and widely used, especially since it is the most versatile approach for retrofitting carbon capture into existing infrastructure [21]. However, the main challenge with this process is the high energy for separating the CO_2 from the flue gas due to the lower concentrations of CO_2, which reduces the capture efficiency. With an estimated CO_2 removal of 90%, post-combustion requires about 4.14 GJ/t-CO_2 [23].

For the scope of the project, only post-combustion carbon capture is applicable since this sort of technology can be retrofitted to existing plants with CO_2 emissions such as cement and pulp plants. Figure 11 below outlines the types of post-combustion carbon carbon capture.

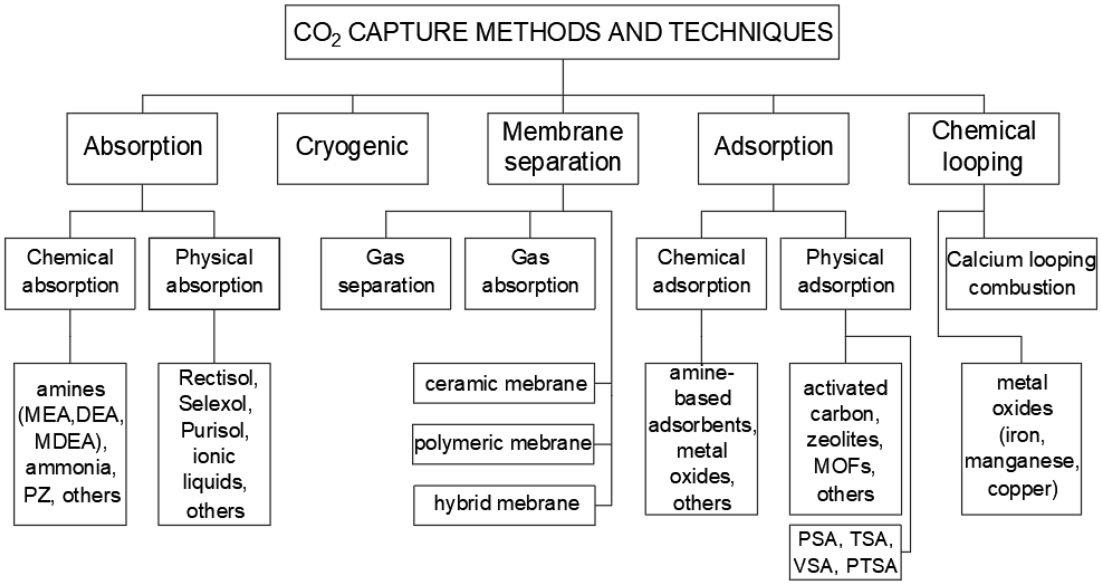

Figure 11: Post combustion carbon capture technologies [24].

Selecting a suitable post-combustion carbon capture technology depends on many factors such as processing scale, flue gas concentration, operating costs, and technological maturity. These factors, along with others, are discussed in detail below.

3.1.1 Absorption

One of the most technologically mature processes for carbon capture is absorption [25]. This type of carbon capture process takes place in two main steps: absorption and desorption. Absorption is the first step where the CO_2 from the industrial flue gas is absorbed into a solvent. The output from the absorber unit is a purified gas stream, containing near zero

CO_2 concentration, and a CO_2-rich solvent stream. Stripping, or desorption, is the second step where the CO_2-rich solvent is regenerated to be recycled back to the absorption column and a near-pure CO_2 stream is recovered to be further processed for storage or utilization.

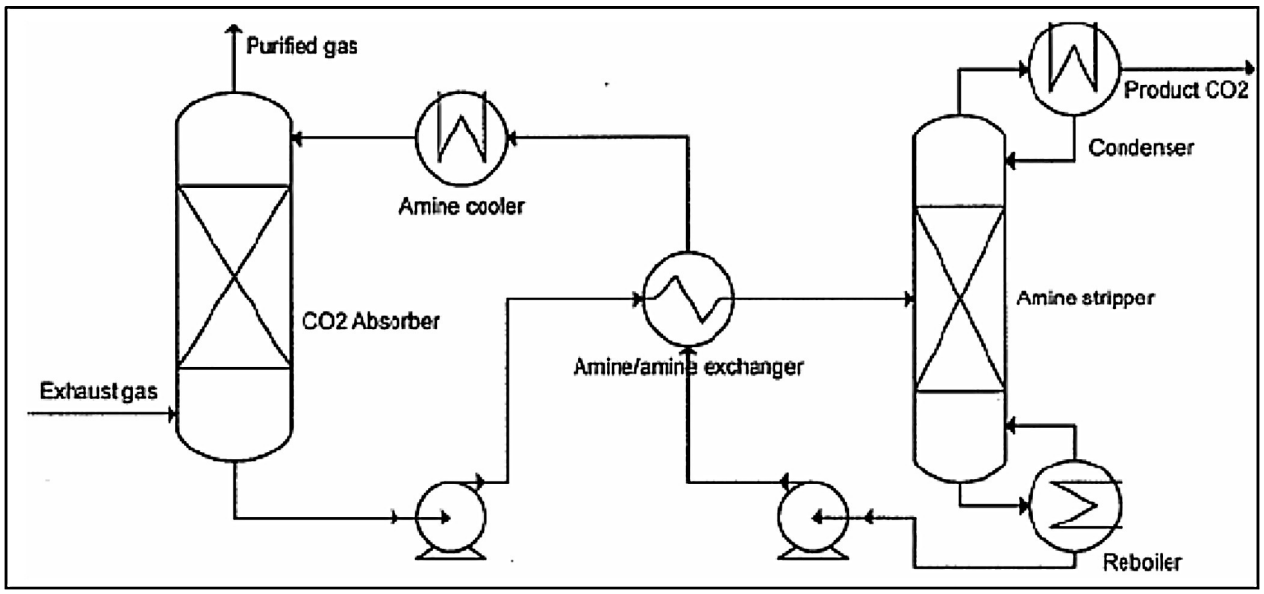

Figure 12: Overview of a typical absorption-desorption process [25].

Some of the important design considerations for absorption-desorption for a CO_2 capture process include the choice of solvent and column type. Each process configuration has benefits and drawbacks in terms of energy consumption, suitability, and operational complexity as discussed below.

Solvents

There are two main types of solvents for absorption-based carbon capture, chemical and physical, depending on the type of interaction between the solvent and absorbed component.

Physical solvents capture CO_2 based on solubility, without a chemical reaction. They work well under high pressure, releasing CO_2 when the pressure is reduced. Dimethyl ether of polyethylene glycol (DEPG), used in Selexol, is stable with low volatility and high CO_2 solubility, while methanol used in Rectisol, is highly effective but requires very low temperatures and can be lost to evaporation [26].

Chemical solvents react directly with CO_2 to form compounds that enhance absorption rates. Key examples include amines, ammonia, and salt solutions. Amines such as monoethanolamine (MEA), diethanolamine (DEA), and methyl diethanolamine (MDEA) are common. MEA is often used as a benchmark in 30 wt% aqueous solutions, it's highly reactive but has limitations such as high regeneration energy demands, volatility, and corrosion potential. DEA and MDEA offer lower volatility and regeneration costs but absorb CO_2 more slowly, while piperazine (PZ) is added to amines for faster kinetics and better thermal stability. Ammonia is also effective and requires less energy for regeneration but poses

challenges due to volatility and potential side reactions. Salt solutions, like potassium and sodium carbonates, are cost-effective, low-toxicity options that regenerate easily, although their slower reaction rates limit them at low CO_2 pressures [26].

Mixed solvents blend chemical and physical types to reduce energy costs and increase performance for CO_2 capture in various conditions. The goal is to enhance the strengths of each type of solvent. The selection of an appropriate solvent depends on the characteristics of the flue gas stream being treated [26].

Columns

Absorption columns are designed to maximize liquid-gas contact surface areas in order to promote the mass transfer of a target species, in this case CO_2, between the two phases. There are four main types of columns with different benefits and drawbacks which are therefore suitable for different industrial applications [27–29]. Figure 13 shows the differences in the internal design for various absorbers and Table 6 summarizes the contact methods, advantages, and disadvantages for each type of column.

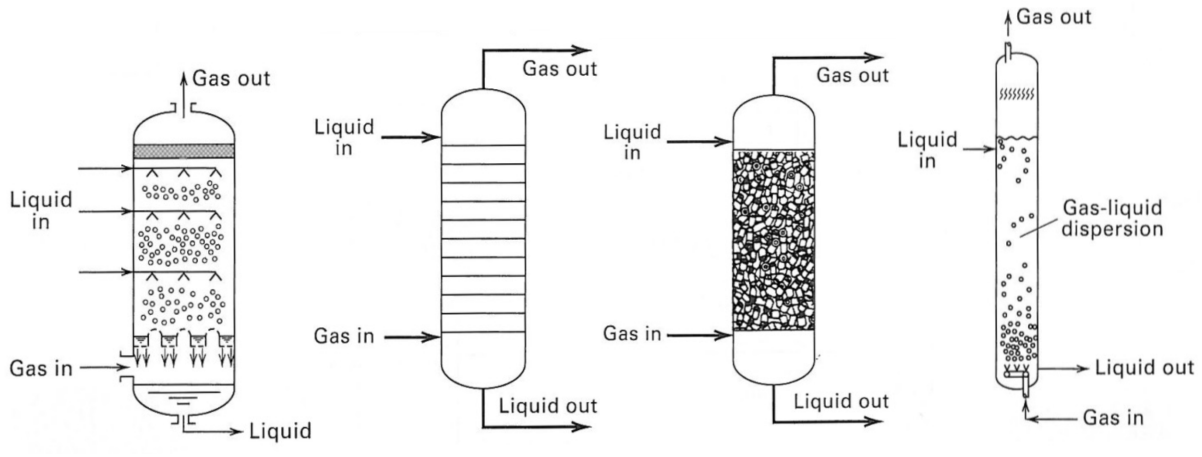

Figure 13: Types of absorption columns (left to right: spray, tray, packed, bubble) [30].

Table 6: Types of absorption columns.

Column Type	Contact method	Advantages	Disadvantages
Packed Column	Packing material: · Structured or random · Materials: metals, plastic, ceramics	· Continuous and high surface area	· Large pressure drop results in higher energy use · Fouling or clogging due to impurities
Tray Column	Horizontal plates in series: · Gas and liquid phases come in contact with each other at equilibrium at each tray	· Better control of mass transfer · Easier maintenance · Lower pressure drop	· Stepwise design results in smaller overall mass transfer efficiency
Bubble Column	Bubbles (flue gas): · Bubbles rise through the liquid and CO_2 is absorbed into the solvent	· Long liquid-gas contact times	· Bubble coalescence decreases the surface area of the bubbles
Spray Column	Droplets (solvent): · Solvent droplets are sprayed and CO_2 is absorbed into the solvent	· Low pressure drop results in lower energy use, simpler maintenance, and lower capital costs · Higher flexibility for gas load variations	· Performance challenges of nozzles such as clogging and uneven spray distribution

Numerical Simulation

Commercial process simulation softwares such as Aspen Plus have been extensively used to model MEA-based chemical absorption for CO_2 capture in order to evaluate different possible industrial scenarios, solvent configurations, and process optimizations. These simulations provide valuable inside into process design, energy consumption, and capture efficiency. Four key publications were selected to extract specific process parameters and operating conditions for various industrial flue gas effluents are summarized in Table 7 below.

Table 7: Examples of Aspen simulations for MEA-based absorption for carbon capture.

	Gervasi et al. [31]	**Parkhi et al. [32]**	**Wells et al. [33]**	**Ren et al. [34]**
Gas Feed				
Source	Cement	Pulp	Iron and Steel	Biomass
Flow Rate	$1.71 \times 10^5\,m^3/h$	73 972 kg/h	130–210 m^3/h	30–100 kg/h
CO_2 (%)	23.75	20.4	10–25	8.4–16.5
H_2O (%)	4.16	30.9	-	-
N_2 (%)	69.71	47.4	-	3.2
O_2 (%)	2.38	1.2	-	-
Solvent Feed				
Flow Rate	$1.698{\times}10^3\,m^3/h$	-	300–1200 kg/h	100–300 kg/h
MEA	30 wt%	30 wt%	35 wt%	30 wt%
Absorber				
Capture Eff.	85%	90%	90–95%	40–88.3%
Pressure	1.2 bar	-	-	1.01 bar
Temperature	40–55°C	-	35–45°C	-
Internal	Bubble Cap Tray	Structured Packing	Structured Packing	Structured Packing
Stripper				
Pressure	1.9 bar	1.8 bar	1–2 bar	1–2.5 bar
Temperature	116°C (inlet)	-	85–110°C	95–120°C
Internal	Bubble Cap Tray	Structured Packing	Random Packing	Structured Packing

These process examples help determine some of the initial specifications for the base case design for the MEA-based absorption process as discussed later in Section 4.1.

3.1.2 Cryogenic

Cryogenic separation is a method to separate CO_2 from gas mixtures by cooling and compressing to low temperatures and high pressures [24]. This process results in the formation of up to 99.99% pure liquid CO_2, which is suitable for transport and storage. This method is most appropriate for gas streams with high CO_2 concentrations, it becomes less efficient at lower concentrations. Cryogenic separation faces some challenges notably since it very energy-intensive due to the cooling and compression required, leading to high operational costs. Additionally, technical issues such as the risk of solid CO_2 clogging equipment also pose significant challenges. Overall, the infrastructure and energy requirements make cryogenic carbon capture less economically competitive compared to other carbon capture methods such as amine scrubbing [23]. Figure 14 shows an example of the process.

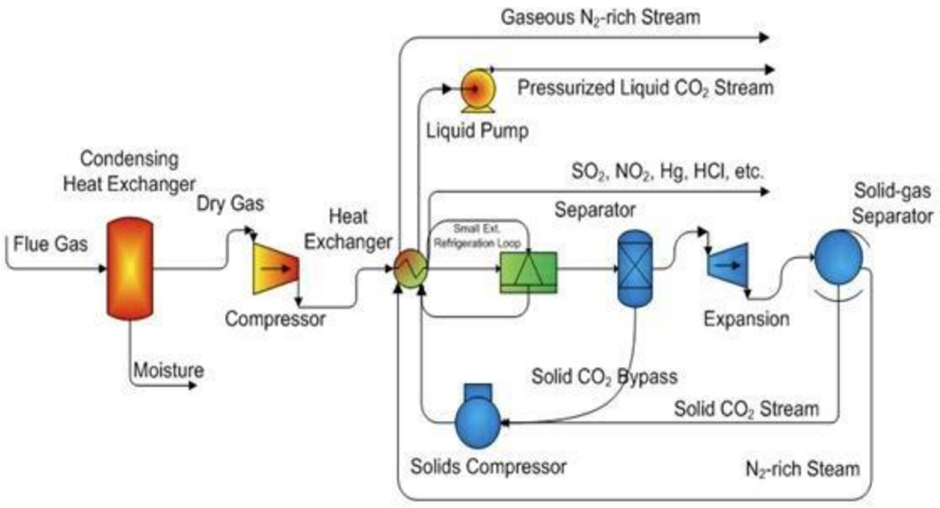

Figure 14: Cryogenic carbon capture [35].

3.1.3 Membrane separation

Membrane separation for carbon capture involves using selective membranes to separate CO_2 from flue gas streams [23]. There are two main types of membrane technologies used: gas separation membranes and gas absorption membranes. Gas separation membranes separate CO_2 from flue gas by passing it through a high pressure membrane, with recovery on the low pressure side. Gas absorption membranes such as solid microporous membranes assist CO_2 absorption into a liquid, offering high removal efficiency while minimizing flooding or foaming [24]. An illustration can be seen in Figure 15.

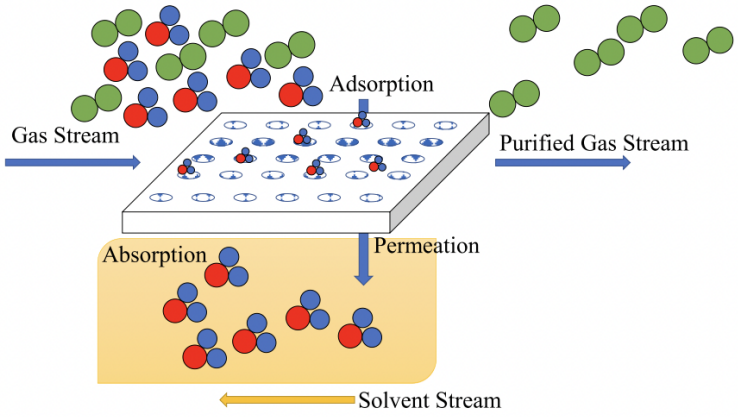

Figure 15: Gas absorption membrane for CO_2 separation [36].

Membrane materials for CO_2 separation must balance high permeance, selectivity, and stability. Polymeric materials dominate because of their low cost, ease of processing, and scalability, with examples including polycarbonates, polyimides, and polysulfones. Inorganic membranes have superior stability but are brittle and costly. Hybrid membranes combine the benefits of both. Advanced designs like thin-film composites are promising for improved performance

in post-combustion CO_2 capture, overcoming the limitations of traditional polymeric membranes [37].

The main advantages of membrane technology is the reduced physical footprint, no chemical additives, no moving parts, and low capital cost. The disadvantages are the lower CO_2 purity produced than in other processes, need for multi-stage processes for high recovery, and low technology readiness level [38].

3.1.4 Adsorption

Adsorption for carbon capture involves binding CO_2 gas molecules to the surface of solid adsorbent materials with high surface areas. This process is versatile due to its high energy efficiency, low waste production, and ability to operate across a wide range of operating conditions, making it scalable for various industrial applications. Some challenges include high sensitivity to impurities such as NO_x and SO_x which can degrade the adsorbent material over time resulting reduced efficiency in the long-term.

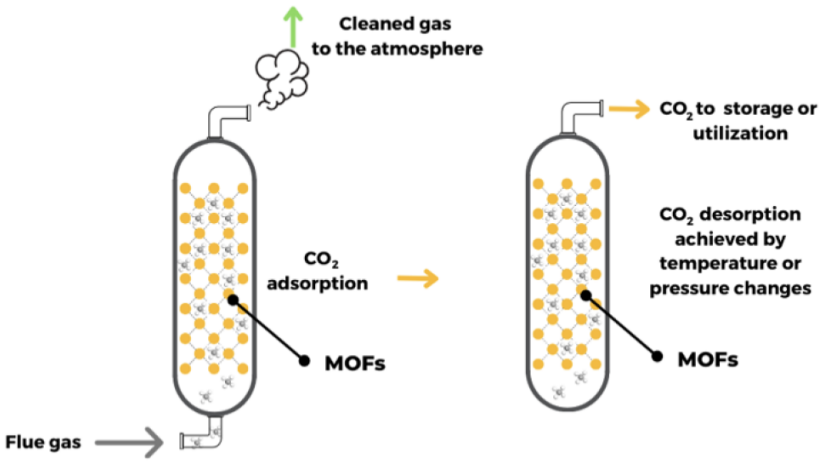

Figure 16: Physical adsorption and desorption process [39].

There are two main types of adsorption processes based on the type of interaction between the solvent and adsorbed component: chemical and physical. The choice of adsorption material depends on the specific application and composition of flue gas. Physical adsorption temporarily binds the gas molecules to the surface via weak intermolecular forces such as van der Waals interactions and is therefore a reversible process and the absorbent material can be regenerated and reused. Some examples of physical adsorbent materials are zeolites, metal organic frameworks, activated carbon, and silica. Generally, physical adsorption is faster. Chemical adsorption permanently binds the gas molecules to the surface via chemical bonds and is therefore an irreversible process. This process has a higher selectivity and capacity than physcial adsorption and therefore is better under lower CO_2 concentrations. Some examples of chemical adsorbent materials are amine-based sorbents, metal oxides, and alkali metals.

3.1.5 Chemical looping

Chemical looping technology captures and separates CO_2 from flue gas based on a metal, most commonly calcium, reversibly reacting between its metal-carbonate form ($CaCO_3$) and its metal-oxide form (CaO) as follows:

$$CaCO_3 \rightleftharpoons CaO + CO_2 \tag{R1}$$

The calcium looping process includes two main steps: carbonation and calcination. Carbonation is where the sorbent, CaO, reacts with CO_2 to produce $CaCO_3$ and thereby reducing the concentration of CO_2 in the gas. This step corresponds to the reverse reaction of R1. Calcination is where $CaCO_3$ is decomposed at high temperatures to regenerate CaO and to produce a concentrated stream of CO_2. This step corresponds to the forward reaction of R1.

This type of technology has a promising potential integration in processes like cement and pulp production where kiln units already use limestone and therefore only the addition of a carbonator unit would be necessary. In cement production, the rotary kiln which is used for the clinker formation step already includes the calcination of $CaCO_3$ from limestone and generates CaO and CO_2. Therefore, there is potential the rotary kiln can be retrofitted to act as a calciner in the calcium looping process and the CaO-rich purge stream has the potential to be used as feedstock for the carbonator [13]. In pulp plants in the causticizing step of the Kraft process, there is a step to calcinate limestone to produce lime, which can therefore directly be implemented to capture CO_2 by adding a carbonator. Figure 17 below shows the suggested implementation for calcium looping for a pulp plant.

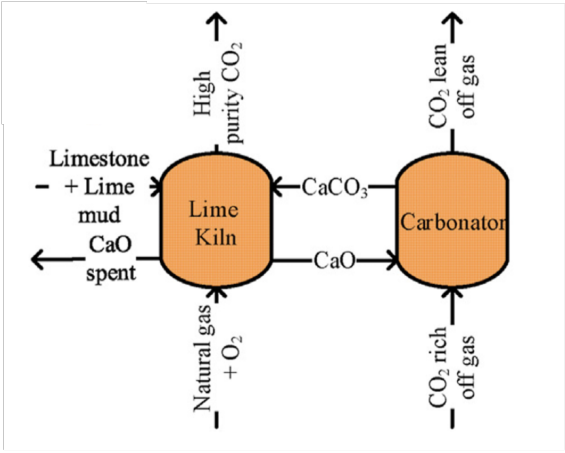

Figure 17: Carbon capture for Kraft process using calcium looping [13].

The direct integration of calcium looping technology into the kiln units is promising however it requires changes to the kiln operating conditions to efficiently use the CaO and $CaCO_3$. Such modifications are beyond the scope of this techno-economic analysis.

3.2 Carbon Storage

Captured CO_2 can be permanently stored underground in bedrock at depths greater than 800 meters, where it exists as a supercritical liquid due to the high pressure [40]. Similar to oil and natural gas, CO_2 can naturally be trapped underground for millions of years. This principle forms the basis of geological CO_2 storage, where carefully managed sites can securely contain injected CO_2 permanently. Reservoirs are porous, permeable rock formations deep underground, onshore or offshore, where fluids or gases like oil, gas, CO_2, freshwater, or brine collect, and when clustered these reservoirs form fields. Suitable CO_2 storage reservoirs are typically found in sedimentary basins, where compacted sediment forms rock, though some igneous formations may also be viable. To securely store CO_2, reservoirs must have an impermeable caprock, or seal, that prevents the gas from migrating beyond its boundaries or reaching the surface. The storage sites can be divided into three categories, saline formations or saline aquifers, depleted oil and gas fields, and unconventional storage resources [41]. Figure 18 illustrates onshore and offshore storage.

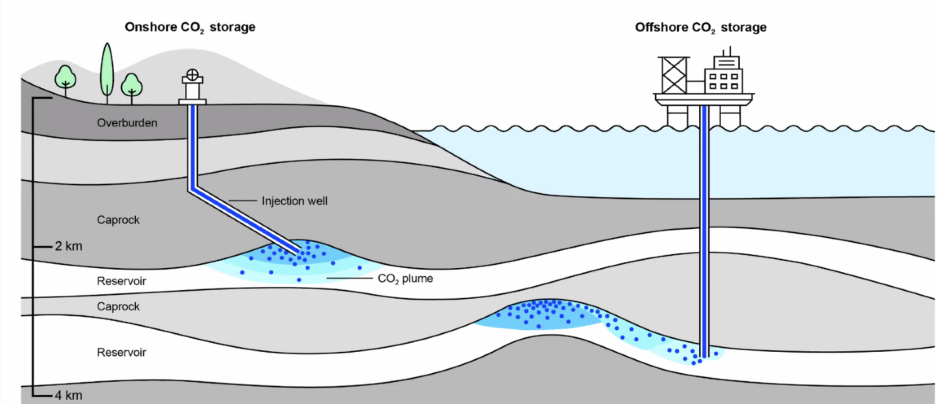

Figure 18: Description of different CO_2 storage types [41].

3.2.1 Storage sites

The first CO_2 storage project to reduce emissions was started in 1996 at Sleipner gas fields in the North Sea in Norway [41]. The Nordic Competence Center for CCS (NORDICCS) identified other potential carbon storage sites in the Nordic region by evaluating subsurface geology, availability, and associated risks. The region offers substantial underground capacity for CCS, with the potential to store 86 Gt of CO_2, equivalent to 554 years of emissions from the Nordic countries. However, Sweden faces challenges compared to Norway, which has oil and gas fields that can be repurposed as CO_2 traps. Sweden's bedrock, both onshore and offshore, primarily consists of low-porosity crystalline rocks such as granite, making it unsuitable for CO_2 storage. Sedimentary rocks like limestone and sandstone, which are better suited for this purpose, are limited in Sweden [42].

The most promising CCS sites in Sweden are located in the southern Baltic Sea and the southwest Skåne region, but these are still in the early investigation stage, with results not expected until 2026 [40, 42]. While deep saline aquifers in southern Sweden offer an estimated

storage capacity of 1.6 billion tons of CO_2, no storage infrastructure has been developed. This has led Sweden to shift its focus from mapping domestic storage potential to relying on near- to mid-term CO_2 storage in Norway, which offers a significantly greater storage capacity of 29 billion tons on its continental shelf [42, 43]. Sweden's dispersed CO_2 capture points and small emission volumes (0.5–2.0 Mt-CO_2/year) make cross-border transport to Norway's extensive storage sites essential. A 2019 resolution by the London Protocol now permits such transport for sub-seabed storage, providing Sweden with a viable pathway to address its CCS challenges by making use of Norway's developed infrastructure and more abundant sequestration capacity [42, 43].

A full-scale CCS value-chain project in Norway, called Longship, is a collaboration between the Norwegian Government and companies to initiate CCS by 2024 [43]. One aspect is the Northern Lights project which manages the transport and permanent storage of CO_2. Northern Lights will provide infrastructure for industry emitters in Norway and Europe. The aim is to contribute to establishing a commercial CCS market in Europe [44]. The Northern Lights will transport and store CO_2 from European industries starting from 2026 [45]. Another project that offers extensive storage for industries, is the Danish project Greensand which will be stored in the North Sea. The project is planned to be operational in early 2026 and offer the storage of CO_2 from Danish biomethane productions [46].

3.2.2 Transport

Once captured, the CO_2 is to be transported from the plant where it was captured, to either an onshore or an offshore storage site. If the selected site is offshore, transport by pipeline or ship can be used [47]. Both transport alternatives are considered viable options for large-scale CCS and transport, but the capacity of captured CO_2 and transport distances affect the costs and further, the choice of transport type [48]. The transport of CO_2 using tanker trucks is mainly used for bulk transportation in cryogenic vessels for retail purposes. However, using this type of transportation for geological storage purposes is deemed too expensive [49]. The method of transportation highly affects the compression and conditioning process at the capture site.

Transport by pipeline is typically preferred for shorter distances between the capture plant and the storage site, due to its continuous operation and lower per-unit transport costs over time. Transport by shipping is preferred for longer distances and higher flexibility [50]. In addition, ships become important since many industrial plants are located along the coasts and the permanent injection sites are often offshore as well [49]. Figure 19, shows a concept of a ship-based CCS chain including the capture process, liquefaction, intermediate storage before and after ship transport, and pumping the CO_2 into a suitable final storage site.

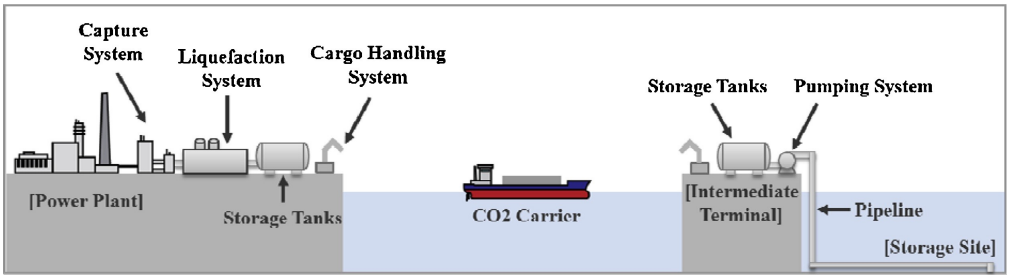

Figure 19: Concept of ship-based CCS chain [47].

.

Another component in the transport chain that might be of importance, regardless of type of transport, is the intermediate storage of CO_2, which is shown in Figure 19. Particularly in cases where one single site stores CO_2 from multiple sources, or if the CO_2 is stored to multiple sites. The intermediate storage provides a steady flow of CO_2 to the storage sites, which is significant for maintaining a safe transmission and operation that is not interrupted at the storage site. Intermediate storage would also perform as a buffer between the capture and permanent storage process in cases of regular or unforeseen maintenance at the storage site [49]. This storage solution also provides a simple technical solution regarding ship transport, since they do not need to be dimensioned for offshore offloading of CO_2 [51].

3.2.3 Compression

The conditions for transport in pipelines and ships differ from each other. Pipelines operate at supercritical pressure and ambient temperature, while ships transport CO_2 in a liquefied state at much lower pressure and temperature, to reduce volume. It takes approximately one-five hundredth of the volume if CO_2 is liquefied compared to gaseous. Figure 20 shows different pressurization approaches, including the conventional approach for pipelines and ships [47, 50, 52].

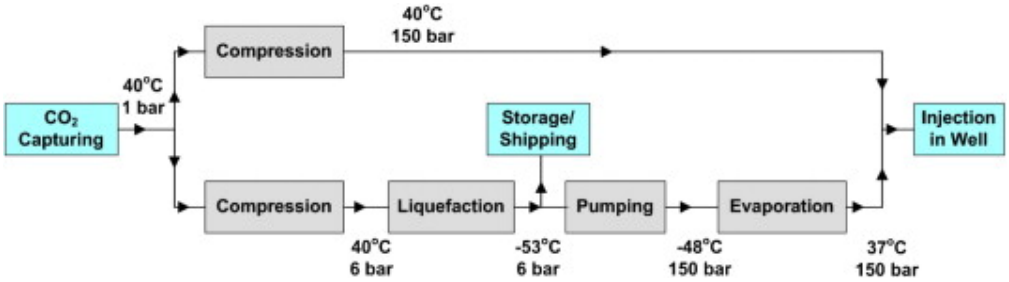

Figure 20: Different CO_2 pressurization approaches [52].

.

CO_2 can be transported in liquid form at a pressure between the triple point (5.18 bar, -56.6°C) to the critical point (31.0 bar, 73.8°C), which can be seen in Figure 21 [53]. After the stripper step in the capture process, CO_2 often has a pressure of 1 bar. It is important to compress the CO_2 above the triple point before the liquefaction. Otherwise, solid CO_2 will be formed during the cooling [52].

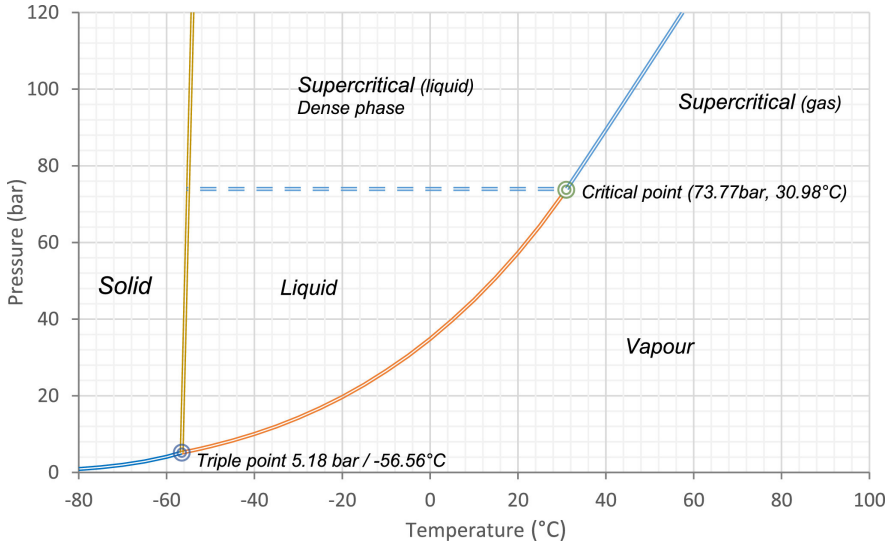

Figure 21: Phase diagram of pure CO_2 [53].

.

The desired inlet pressure is different between onshore and offshore pipelines. While an onshore pipeline requires conditions of 150 bar and ambient temperature, an offshore pipeline operates at 200 bar [48]. Figure 22 shows the flow diagram of conditioning to offshore pipeline transport including four compression stages with intercooling between, combined with dehydration, followed by pumping.

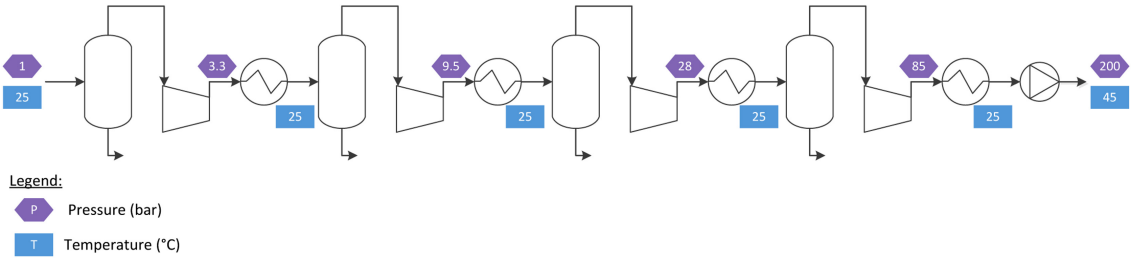

Figure 22: Flow diagram of conditioning to offshore pipeline export process [54].

.

Figure 23 shows a flow diagram of conditioning to shipping export of CO_2 to 6.5 bar and -50°C, using ammonia liquefaction (cooling and expansion). The gas is cooled down to 25°C between the compression stages and the water content is removed [54]. A large refrigeration system is needed to liquefy CO_2 near the triple point, whereas a substantial compression system is required near the critical point. Additionally, as the critical point is approached, the density of the liquefied CO_2 decreases, making transportation near the critical point less advantageous [47]. Furthermore, impurities in the CO_2 may result in higher transport pressures [50]. A higher liquefaction pressure reduces the costs of the liquefaction and pumping systems but increases the costs of storage tanks and CO_2 carriers. The most common liquefaction condition mentioned in literature is 7 bar which corresponds to liquefied petroleum gas (LPG). A study performed a comparison of different liquefaction pressures, where 15 bar was the optimal alternative [47].

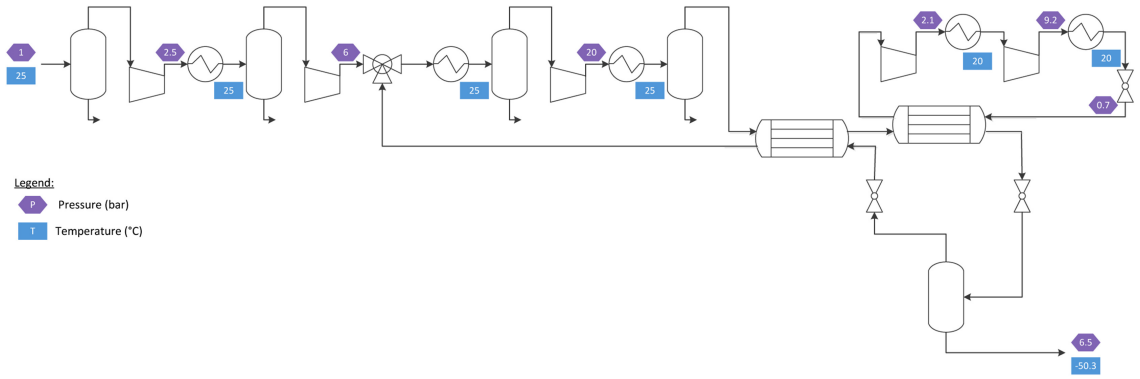

Figure 23: Flow diagram of conditioning to shipping export [54].

.

The most common process designs for liquefying CO_2 are open and closed cycles. For the open cycle, a fraction of the CO_2 is recycled for the liquefaction. In the closed cycle, an external refrigeration cycle is used for the liquefaction [50]. However, it was found the open cycle was unfeasible for CO_2 streams with impurities.

The selection of a storage site plays a pivotal role in determining the appropriate transport alternatives and compression requirements, which in turn shape the overall efficiency and feasibility of the carbon capture process. These interdependencies highlight how different storage scenarios can influence the design and operation of carbon capture and storage.

3.3 Carbon Utilization

Carbon utilization includes a range of technologies and processes aimed to convert CO_2 into valuable products, thereby mitigating its environmental impact and creating economic opportunities. This section explores two major strategies for CO_2 utilization: direct applications, where CO_2 is used in its captured form for various industrial processes, and chemical transformation, in particular methanol synthesis from CO_2 through a catalytic process. Each of these approaches has distinct benefits and challenges, and their integration into large-scale industrial applications is critical for achieving carbon neutrality goals.

In the following subsections, key pathways for direct utilization of CO_2 will be discussed, including enhanced oil recovery and supercritical CO_2 applications in food and materials processing. Then, the chemical transformation pathway is explored, focusing on the hydrogenation of CO_2 to methanol, which holds promise as a versatile solution for both emissions reduction and energy storage.

3.3.1 Direct Utilization

McLaughlin et al. have conducted an extensive review of various technologies to utilize captured CO_2 [55]. There are numerous potential uses for purified CO_2, including biofuel production, pharmaceutical manufacturing, fuel cell creation, and enhanced oil recovery. However, many of these utilization processes are not economically viable on a large scale.

At present, enhanced oil recovery (EOR) is the most commonly implemented application for captured CO_2 and remains the most cost-effective utilization option [56].

Enhanced Oil Recovery

EOR involves injecting CO_2 into depleted oil or gas reservoirs to enhance production and prolong the life of the field [56]. As CO_2 is injected into the oil-bearing zone, it mixes with and displaces the oil, increasing pressure in the producing intervals and reducing the oil's viscosity to boost extraction capacity [57]. While the operational procedures of EOR are similar to CO_2 injection in saline reservoirs, not all injected CO_2 is stored in the reservoir. Some CO_2 remains trapped underground, but the primary goal of EOR is to extract more oil and gas. Once decommissioned, EOR fields could potentially be repurposed as permanent CO_2 storage sites [58]. When assessing the effectiveness of EOR for CO_2 mitigation, emissions associated with continued oil production must be considered in the life cycle assessment (LCA)—the net CO_2 removal through this process should be reviewed for a more comprehensive assessment.

The CO_2 reuse market, particularly in the U.S., is largely driven by EOR activities, with the majority of these operations based in West Texas [59]. Current demand for CO_2 stands at 62 t-CO_2/year, but some estimates suggest this could increase to as much as 500 t-CO_2/year [59]. A technoeconomic model has shown that Recycle–CCS–EOR (RCE) projects could reduce carbon emissions by 54.7% more than traditional EOR, though economic feasibility depends on market conditions [60]. The main barrier to expanding CO_2 utilization is the lack of adequate transportation infrastructure [55].

Supercritical CO_2 Applications in Food and Materials Processing

Supercritical CO_2 (SC-CO_2) extraction has emerged as a versatile and efficient technology in the food industry, offering a sustainable alternative to conventional methods. This process exploits the unique properties of supercritical CO_2, such as its tunable density and solvating power, to extract bioactive compounds, oils, and other valuable components from food and agricultural materials. SC-CO_2 is widely preferred due to its non-toxic, non-flammable, and environmentally friendly nature, making it ideal for producing high-purity products without residual solvents. Its applications range from extracting essential oils and flavors to recovering bioactive compounds from by-products. Additionally, SC-CO_2 demonstrates the potential for inactivating microbes and enzymes, contributing to food preservation. Recent advancements in scaling up SC-CO_2 processes have further enhanced its industrial relevance, solidifying its role in sustainable food processing [61].

SC-CO_2 has also found applications in the recovery of metals, particularly in addressing environmental challenges and resource sustainability [62]. Utilizing supercritical CO_2, typically with suitable co-solvents, enables selective leaching of metal ions from complex matrices such as electronic waste, mining residues, and industrial catalysts [63–65]. This method has advantages over traditional hydrometallurgical and pyrometallurgical techniques, as it reduces chemical waste, energy consumption, and environmental contamination. Metals such as gold, platinum, and rare earth elements can be efficiently recovered using SC-CO_2 due to their tunable solvating properties. The process is increasingly being explored for sustainable urban

mining, aligning with the recent growth of the battery industry and circular economy principles, and offers potential for industrial scalability with advancements in solvent formulations and process optimization.

3.3.2 Chemical Transformation - Hydrogenation to Methanol

Among various pathways for CO_2 utilization, methanol synthesis stands out as one of the most promising options due to its versatility and potential for large-scale application. Methanol can serve as a valuable feedstock for the production of chemicals such as olefins and can also be used as a fuel or energy carrier, thus offering a sustainable solution for both emissions reduction and energy storage. Recent studies have focused on optimizing the hydrogenation of CO_2 to methanol, aiming to improve kinetic model accuracy, process efficiency, and cost-effectiveness, while enhancing overall sustainability.

Bowker's review emphasizes the importance of CO_2 as a key carbon source for methanol synthesis [66]. While industrial methanol production typically uses CO as the carbon feedstock, there is growing interest in developing processes that directly convert CO_2 and hydrogen into methanol. This shift is driven by the need for more sustainable, carbon-neutral production methods. Bowker also highlights ongoing efforts to implement these processes on a commercial scale, with a demonstrator plant currently under construction to showcase the viability of CO_2-based methanol synthesis.

Chemistry
The chemistry in methanol synthesis from CO_2 involves three catalytic reversible reactions: CO_2 hydrogenation (R2), CO hydrogenation (R3), reverse water-gas-shift reaction (R4). $Cu/Zn/Al_2O_3$ catalysts are the most widely used and a lot of data on their density, porosity, and particle dimensions have been reported [60, 67–69].

$$CO_2 + 2\,H_2 \rightleftharpoons CH_3OH + H_2O \tag{R2}$$
$$CO + 3\,H_2 \rightleftharpoons CH_3OH \tag{R3}$$
$$CO_2 + H_2 \rightleftharpoons CO + H_2O \tag{R4}$$

Nyári et al. [70] compared different kinetic models for CO_2 hydrogenation, reported details on how to implement them in Aspen Plus, and investigated the impact of model selection on the results of technoeconomic analyses. Most of the kinetic models found in the literature assume that CO_2 is the main source of methanol, reducing the system to only two reactions: R2 and R4.

The exothermic nature of the overall reaction imposes an optimization challenge, where there is a trade-off between reaction kinetics and thermodynamic equilibrium limit—the maximum single-pass conversion is limited below 30% within the range where the reaction rate is sufficiently fast. However, recycling unreacted gas with the molar recycle ratio higher than 5 can work around this limit, yielding overall CO_2 conversion up to 97–99% [71].

Process

Although there is no existing commercial-scale CO_2 hydrogenation process reported at the moment, numerous studies on the design and optimization of the process have been published. As shown in Figure 24, the process typically involves three main stages: catalytic hydrogenation in a reactor, vapor-liquid separation through flash distillation, and purification via distillation. Three key publications were selected to extract specific process parameters and operating conditions: Van-Dal and Bouallou [68], Battaglia et al. [60], and Yusuf and Almomani [69].

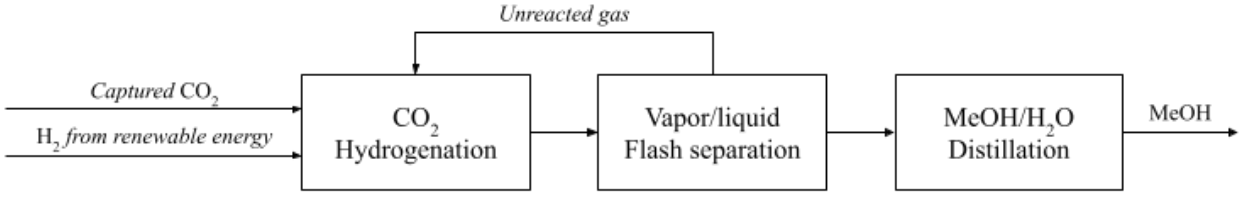

Figure 24: MeOH process.

Van-Dal and Bouallou [68] proposed a process that integrates CO_2 capture via chemical absorption from flue gases, with hydrogen produced through water electrolysis using carbon-free electricity. The methanol plant provides 36% of the thermal energy needed for CO_2 capture, reducing the overall energy costs associated with the capture process. Their analysis indicated a potential CO_2 abatement of up to 1.6 tons per ton of methanol produced. In their optimized process, parallel heat integration was implemented: a fraction of the hot product stream preheats the reactor feed, and the remainder supplements the heating duty of the reboiler in the distillation column and preheats the liquid feed to the column.

Battaglia et al. [60] focused on the integration of CO_2 capture, water electrolysis, and methanol synthesis, developing a comprehensive process model to simulate a system that captures CO_2 from a coal-fired power plant and converts it into methanol using renewable hydrogen. The authors applied pinch analysis to optimize thermal integration, resulting in significant energy savings and improved plant efficiency. Notably, the process involves serial heat recovery, where the entire hot process stream is used to preheat the reactor feed and subsequently the liquid feed to the distillation column. Their process, operating at an overall efficiency of 37.22%, demonstrated the potential for reducing methanol production costs to a range of €565–€2 706 per ton, depending on the energy source used for electrolysis.

Yusuf and Almomani [69] studied CO_2 catalytic hydrogenation with a $Cu/ZnO/Al_2O_3$ catalyst at 70 bar and 210°C, achieving 95.66% CO_2 conversion and over 99% methanol yield. They optimized the system using Aspen Energy Analyzer V11 for pinch analysis with a 5°C $T_{\min}$, balancing reduced utility costs and increased capital costs from additional heat exchangers.

These studies provide important information on the key process units and operating conditions for CO_2 hydrogenation to methanol. Table 8 summarizes the process parameters used

in the three studies, which will serve as the basis for our initial base case simulation.

Application and Quality Standard

Methanol is an incredibly versatile substance used in a wide range of everyday household products, essential automotive components, and the production of other valuable chemicals. Increasingly recognized as a clean and sustainable fuel, methanol stands out for its clean-burning characteristics, which reduce emissions and enhance fuel efficiency in land and marine vehicles. When produced from renewable sources like captured CO_2 or waste, methanol becomes a carbon-neutral fuel, aligning with climate policies aimed at reducing greenhouse gas emissions.

International Methanol Producers & Consumers Association (IMPCA) has published detailed quality specifications for methanol as a marine fuel [72], which is the most widely accepted quality standard for MeOH production. Their recent standard recommends the dry-basis methanol purity $> 99.85\,\mathrm{wt\%}$ and water content $< 0.1\,\mathrm{wt\%}$.

Table 8: MeOH synthesis: Detailed process parameters.

	Van-dal and Bouallou [68]	**Battaglia et al. [60]**	**Yusuf and Almomani [69]**
Feed CO_2			
Pressure	1 bar	1 bar	47.63 bar
Temperature	25°C	25°C	12.3°C
Flow rate	88.0 t/h	88.0 t/h	76.46 kmol/hr
Source	Coal power plant	Coal power plant	Cryogenic biogas upgrading process
Feed H_2			
Pressure	30 bar	30 bar	20 bar
Temperature	26°C	26°C	25°C
Flow rate	12.1 t/h	12.1 t/h	535.22 kmol/hr
Source	Water electrolysis	Water electrolysis or natural gas reforming	Water electrolysis
Reactor			
Inlet pressure	75.7 bar	65 bar	75.7 bar
Inlet temperature	210°C	250°C	210°C
Catalyst			
Catalyst type	$Cu/ZnO/Al_2O_3$	$Cu/ZnO/Al_2O_3$	$Cu/ZnO/Al_2O_3$
Catalyst weight	44 500 kg	-	-
Catalyst density	1 775 kg/m^3	1 560.7 kg/m^3	1 775 kg/m^3
Particle diameter	5.5 mm	-	5.5 mm
Bed porosity	0.4	0.39	0.4
Pressure drop	Ergun equation	-	Ergun equation
Thermo model	RKS w/ modified Huron-Vidal mixing rules for high P NRTL-RK for low P	-	RKS
Kinetic model	Vanden Bussche and Froment [**vanden˙steady**]	Other	Graaf
MeOH Purity	99%	99%	>98%

The specifications in Table 8 are used to determine some of the initial specifications for the CO_2 hydrogenation process as discussed in Section 4.3.1.

4 Process Design

This section presents the proposed process design for each sub-process within the overall CCUS framework including capture, storage, and utilization. These processes are designed based on the literature review in Section 3. The proposed processes are simulated in Aspen-Plus v14.

4.1 Carbon Capture

As discussed in Section 3.1, there are many different approaches to capture carbon from industrial flue gases. The most technologically advanced process is MEA-based absorption [23]. MEA was chosen with regards to the design specifications. The objective was to capture up to 90% of the CO_2 from the emission streams of the plants. Of all the available methods of CO_2 removal absorption is the most mature when most research is done on the subject.[73]

The most common method of absorption is 30 wt% MEA in an aqueous solution. This method of cleaning the in coming flue gas was chosen for several reasons. The method of choice has to be able to operate at industrial scale, this is true for MEA absorption as it is highly solvable in water which is key given the scale. Furthermore, to decrease the cost of operation the solvent has to be easily recyclable which is also true for MEA with only a small percentage being lost each cycle depending on the conditions in the system [73].

MEA reacts with CO_2 in an exothermal kinetic reaction. The reaction produces heat as a result. The mechanism of how MEA and CO_2 react in the absorber can be seen in reaction 5.

$$\mathrm{MEA} + \mathrm{CO_2} + \mathrm{H_2O} \longrightarrow \mathrm{MEACOO^-} + \mathrm{H_3O^+} \tag{R5}$$

In the sStripper the reaction is revered as seen in reaction 6.

$$\mathrm{MEACOO^-} + \mathrm{H_3O^+} \longrightarrow \mathrm{MEA} + \mathrm{CO_2} + \mathrm{H_2O} \tag{R6}$$

There are also several more reactions present in the system that happen at equilibrium and kinetically. These reactions can be seen below [74].

$$\mathrm{MEAH^+} + \mathrm{H_2O} \rightleftharpoons \mathrm{MEA} + \mathrm{CO_2} + \mathrm{H_2O} \tag{R7}$$
$$2\,\mathrm{H_2O} \rightleftharpoons \mathrm{H_3O} + \mathrm{OH^-} \tag{R8}$$
$$\mathrm{HCO_3{}^-} + \mathrm{H_2O} \rightleftharpoons \mathrm{CO_3^{2-}} + \mathrm{H_3O} \tag{R9}$$
$$\mathrm{CO_2} + \mathrm{HO^-} \longrightarrow \mathrm{HCO_3^-} \tag{R10}$$
$$\mathrm{HCO_3{}^-} + \mathrm{H_2O} \longrightarrow \mathrm{CO_3^{2-}} + \mathrm{H_3O^+} \tag{R11}$$

4.1.1 Proposed Capture Process

The conditions in the given system are dependent on the size of the different components in the system as well as the inlet streams. The main components in the system are: absorber, heat exchanger, and stripper. Where mainly the absorber and stripper are of concern. The

inlet stream in question is the flue gas and lean solvent entering the absorber. The flue gas entering the system is based on Naturvårdsverket's report of the emissions from both Slite and Korsnäs. This means the system for CO_2 capture is almost devoid of NO_x and SO_x as the emission streams for both industries have already been treated according to Swedish regulations [75]. The liquid-to-gas ratio was determined mainly through sensitivity analysis and was approximately 0.3 mol CO_2 per mol MEA. Due to the space limitations described in Section 2.3 and the need to optimize both CO_2 capture and MEA recovery, the system was designed to minimize its footprint. This resulted in a plant layout that prioritizes height over width. The incoming flue gas is directed to an absorption column, whose height and diameter were determined through sensitivity analysis to ensure effective CO_2 capture while avoiding operational issues such as flooding. The absorber includes several stages optimized for CO_2 capture rather than profitability, and it uses metal packing material chosen based on a literature review of contemporary systems [76].
The conditions in the absorber were decided partly through a sensitivity analysis and partly through a literature study. Through literature, a good starting point was determined and it was optimized through sensitivity analysis.

The stripper, like the absorber, is also a packed column using the same type of material for consistency and efficiency. It is designed with multiple stages to maximize CO_2 release, with dimensions and operational parameters optimized to prevent flooding. The pressure remains consistent throughout the system, adapted to meet the needs of different applications. To ensure separation in the stripper a kettle re-boiler is used to increase the overall temperature of the solvent to reverse the equilibrium between MEA and CO_2. Between the absorber and stripper, a heat exchanger is employed to precondition the flow, improving energy efficiency. The complete model is seen in Figure 25.

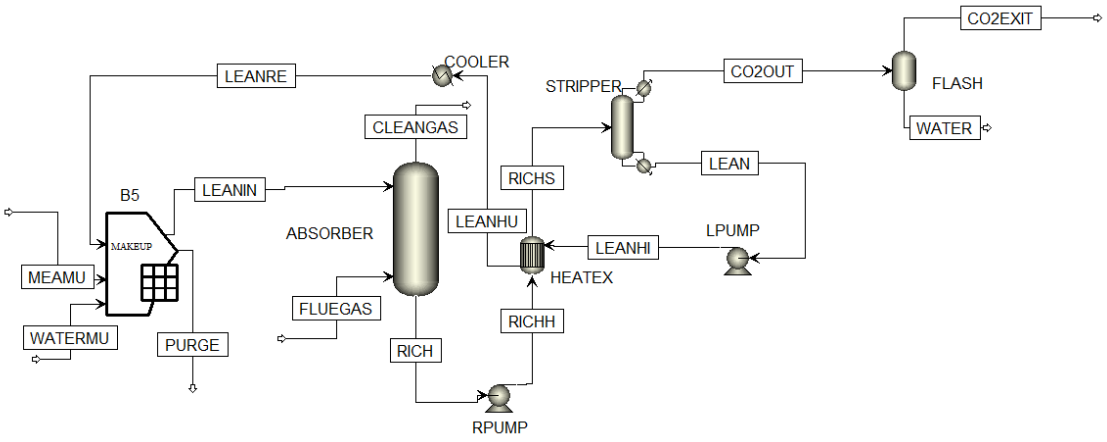

Figure 25: CCS schematic.

4.1.2 Simulation Implementation and Results

The key assumptions and unit input specifications for simulating the process in AspenPlus are summarized in Tables 9 through 11.

Table 9: Assumptions for AspenPlus simulation implementation for carbon capture.

Assumption	**Value**	**Reference**
Aspen package	V14.0	-
Equation of State	ENTL&RK	[74]
G/L ratio	0.3	[73]
Packing material	Flexipac	[73]
Calculations	Equilibrium	[73]
Thermal degradation	None	[73]
Flue gas temperature	18°C	[73]
Solvent temperature	40°C	[73]

Table 10: Composition of the flue gases for Carbon Capture process (t/h).

Molecule	**Cement**	**Pulp**
CO_2	130.75	172.64
O_2	53.89	5.59
N_2	348.80	193.37
H_2O	72.26	81.07
Total	605.70	452.67

Table 11: Composition of solvent stream for Carbon Capture process (t/h).

Molecule	**Mass flow (cement)**	**Mass flow (pulp)**
Water	1410.83	1074.74
MEA	628.15	459.67

Table 12: Aspen Plus input specifications for carbon capture process.

Block	Specification	Input (Cement)	Input (Pulp)
Absorber	Top stage pressure	1.2 bar	1.2 bar
	Number of stages	6	6
	Height	40 m	35 m
	Diameter	12 m	8 m
Heat exchanger	Hot outlet temperature	80°C	80°C
Stripper	Top stage pressure	1 bar	1 bar
	Number of stages	20	20
	Reboiler ratio	0.9	0.9
	Height	35 m	30 m
	Diameter	18 m	17 m
Flash Drum	Outlet Temperature	6°C	6.84°C
Cooler	Outlet Temperature	40°C	40°C

Tables 12 through 15 present the simulation results including the unit energy consumption, capture rates, and cleaned flue gas composition.

Table 13: Aspen Plus output results for carbon capture process.

Block	Result	Output (cement)	Output (pulp)
Absorber	Temperature	69.43°C	68.13°C
Heat exchanger	Heat duty	70.39 MW	55.02 MW
	Exchanger area	8 012.22 m^2	5 445.56 m^2
Stripper	Bottom stage temperature	103.45°C	103.23°C
	Reboiler heat duty	1 210.84 MW	667.15 MW
Flash Drum	Heat duty	−31.39 MW	−55.19 MW
Cooler	Heat duty	−118 457.96 MW	−117.10 MW

Table 14: Results from the CO_2 captured unit.

Result	Cement	Pulp
CO_2 capture rate (t-CO_2/hr)	161.21	122.88
CO_2 capture efficiency (%)	93.43	93.99
Specific reboiler duty (GJ/t-CO_2)	27.02	25.57

Table 15: Composition of the clean gas from absorber.

Molecule	Cement (mol%)	Pulp (mol%)
MEA	8.85×10^{-5}	7.32×10^{-5}
CO_2	3.8×10^{-6}	4.94×10^{-6}
N_2	0.84	0.91
H_2O	0.05	0.06
O_2	0.11	0.02

As seen most CO_2 is captured with only a small fraction leaving with the clean gas. Some CO_2 leave with the purge stream that balances the system's solvent composition.

4.2 Carbon Storage

As discussed in Section 3.2, for the captured carbon to be stored it must be further conditioned to meet specific pressure and temperature for safe and efficient transportation to a storage site. These conditions vary with the transportation type and specific requirements for the receiving storage site. For this project, storage with Northern Lights in Norway is the most suitable option due to its proximity to Sweden, robust infrastructure including transport of CO_2 on their ships, and large capacity for CO_2 storage. Their facility has recently begun operations with CO_2 emissions from their partner cement plant and they are expected to accept other industrial CO_2 by 2025, which is within this project timeline [44].

The specific storage condition requirements for the Northern Lights ships to transport the CO_2 from the capture plant to their injection site are outlined in Table 16 below. The proposed conditioning process to obtain these conditions and the corresponding Aspen simulation implementation are described in the following sections.

Table 16: Target conditions for CO_2 storage at Northern Lights [44].

Parameter	Specifications
Temperature	-30.5 to -26.5°C
Pressure	13 to 15 bar(g)
Density	< 1100 kg/m^3
CO_2 Purity	99.81 mol%

4.2.1 Proposed Conditioning Process

To achieve the target conditions described in Table 16, several compression and cooling steps are combined based on established storage processes [54, 77]. First, the captured CO_2 gas is incrementally compressed with cooling after each stage to increase the pressure while limiting the temperature rise and removing the water. In the first series of compressions, the pressure of the gas is increased from 1 to 15 bar through three identical compressors. The intermediate pressures are calculated using the compression ratio which is defined as follows:

$$R = \left(\frac{P_{\mathrm{D}}}{P_{\mathrm{S}}}\right)^{\frac{1}{n}} \tag{1}$$

where P_{D} and P_{S} are the discharge and suction pressures (bar), and n is the number of stages. The compression ratio should be between 1.2–3 to balance mechanical limitations and thermodynamic efficiency [78].

Next, ammonia refrigeration is used to cool the CO_2 to subzero temperatures in a heat exchanger. The ammonia refrigeration process is in a closed loop and the ammonia is regenerated by compression, cooling, and expansion. Finally, the cooled CO_2 is expanded through a Joule-Thompson valve where the pressure drop reduces the temperature and pressure and results in the phase change into a liquid-gas equilibrium. After expansion, the CO_2 is separated in a flash drum. The liquid CO_2 stream is sent to intermediate storage and the gaseous CO_2 is recycled back into the process to minimize waste and to assist in pre-cooling the warmer CO_2 stream. The proposed process is shown in Figure 26 below.

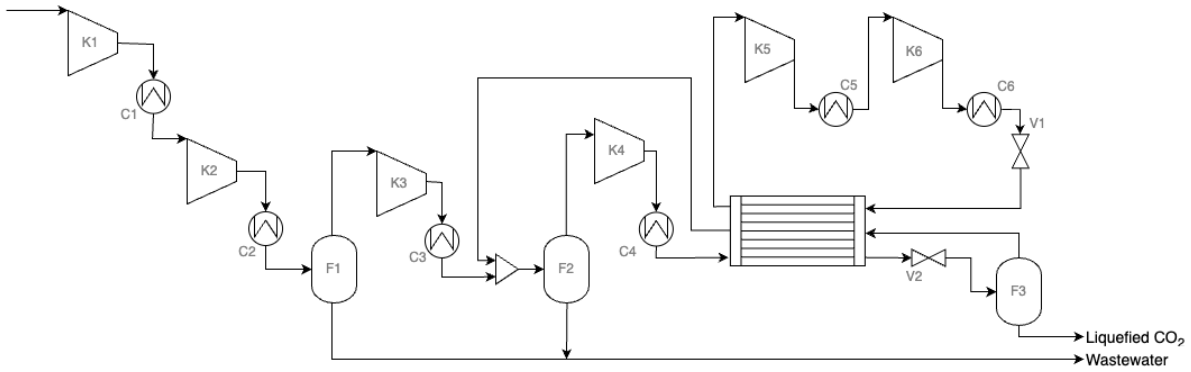

Figure 26: Proposed process for CO_2 conditioning for shipping.

4.2.2 Simulation Implementation and Results

The key assumptions and unit input specifications for simulating the process in Aspen Plus V14 are summarized in Tables 17 and 18 below.

Table 17: Assumptions for Aspen simulation implementation for carbon storage.

Assumption	**Value**	**Reference**
Equation of State	Peng-Robinson	[54, 77]
Compressor isentropic efficiency	0.75	[77]
Compressor mechanical efficiency	0.90	[78]
Compression ratio range	1.2-3	[54, 77, 78]

Table 18: Aspen Plus input specifications for storage conditioning process.

Block	**Specification**	**Input**
Compressors[a]		
K1, K2, K3	Pressure ratio	2.47
K4	Discharge pressure	25 bar
K5, K6	Pressure ratio	2.64
Flash vessels[b]		
F1	Pressure	6.09 bar
F2, F3	Pressure	15 bar
Coolers		
C1	Temperature, pressure	35°C, 2.47 bar
C2	Temperature, pressure	35°C, 6.09 bar
C3	Temperature, pressure	30°C, 15 bar
C4	Temperature, pressure	30°C, 25 bar
C5	Temperature, pressure	35°C, 5.3 bar
C6	Temperature, pressure	35°C, 14 bar
Heat exchanger[c]		
E1	Hot CO_2 stream outlet temperature	−12°C
	Cold CO_2 stream outlet temperature	−10°C
Expanders		
V1	Discharge pressure	2 bar
V2	Discharge pressure	15 bar

[a] The isentropic efficiency is 0.75 and the mechanical efficiency is 0.90 for all compressors.
[b] The duties are zero for all flash vessels.
[c] The heat exchanger involves three streams and therefore requires two outlet stream specifications.

The resulting streams for the streams entering and leaving the overall process are summarized in Table 19. The flow rate of the ammonia refrigerant in the closed loop is 5.2×10^4 and 4.0×10^4 kg/h for the cement and pulp plants respectively.

Table 19: Product and waste stream data for compression for cement and pulp plants.

Plant Type	**Cement**		**Pulp**	
Stream	Product	Waste	Product	Waste
Phase	L	L	L	L
Temperature (°C)	−28.3	19.1	−28.3	18.3
Pressure (bar)	15	1	15	1
Flow Rate (t/h)	150	0.55	120	0.46
CO_2 (mol%)	99.83	0.01	99.82	0.01
H_2O (mol%)	0.13	99.99	0.15	99.99
Other (mol%)	0.030	-	0.3	-

The product streams from the cement and pulp plants meet the specifications required for shipping with Northern Lights outlined in Table 16.

4.2.3 Proposed Intermediate Storage and Transportation Logistics

Once the CO_2 is compressed to the desired conditions, it is stored in intermediate storage vessels onsite until the ships from Northern Lights arrive to transport the liquefied CO_2 to their permanent storage site. The total travel time between the industrial facility and the Northern Lights facility is calculated as follows:

$$\tau = \frac{D_{NL}}{v_{ship}} \times 2 + \tau_{load} + \tau_{unload} \tag{2}$$

where τ is the total round trip transportation time (days), D_{NL} is the one-way distance to the Northern Lights facility which is 1 415 and 1 770 km for cement and pulp plants respectively [79], v_{ship} is the average speed of the ship which is 15 knots (27.78 km/h) [80], and τ_{load} are the τ_{unload} CO_2 loading and unloading times which are both 1 day each [80]. Based on these parameters, the total transportation time for a round trip is calculated and summarized in Table 20.

The Northern Light ships each have capacities of 7 500 m^3 [44]. To accommodate these shipments, intermediate storage must be sufficient to allow for uninterrupted operations. The recommended onsite storage capacity is 200% of the ship capacity, which corresponds to three cylindrical intermediate storage vessels, each with a volume of 5 000 m^3 [80]. These vessels are made from a high-strength steel alloy (A-517) which is suitable for the temperature and pressure of the liquefied CO_2. Based on the production rate of CO_2 summarized in Table 19, the time to produce the capacity of CO_2 which one ship can contain is summarized in Table 20.

Table 20: Summary of intermediate storage and transportation logistics.

Logistic	Cement	pulp
Distance (km)	1 415	1 770
Travel time (days)	6.2	7.3
Production time per ship capacity (days)	2.2	2.7

Since the CO_2 production duration is shorter than the round-trip travel time of the ships, the pick-up schedule must be optimized to prevent CO_2 production from exceeding the transportation capacity.

4.3 Carbon Utilization

As discussed in Section 3.3.2, methanol synthesis was chosen as our carbon utilization method. In this section, process simulation methods and results for the CO_2 hydrogenation to methanol will be presented. Reflecting the two different sources of captured carbon, two separate processes were designed and scaled to them, with most of the differences in the reactor and the distillation column dimensions.

The purification steps in the process were designed to meet the compositional specifications recommended by IMPCA [72]. The final processing of the purified methanol was not included in the simulation—the exit condition of the product stream from the distillation column is the final product condition (1.5 bar, 67.7 °C).

4.3.1 Proposed Utilization Process

A flowsheet for the simulation of the methanol synthesis process is given in Figure 27. First, captured CO_2 and H_2 are fed into the system with H_2/CO_2 molar ratio of 3. The mixture of unreacted gases and fresh feed streams is preheated by the hot product stream at E1, and fed to the reactor (R1). Then the product stream is separated by two consecutive flash vessels operating at high and low pressures. Finally, the separated liquid stream is further purified in the distillation column (C1) while the unreacted gas is compressed and fed back to the feed.

4.3.2 Simulation Implementation and Results

The key assumptions in the process simulation are summarized in Table 21 below. Based on the literature review, Peng Robinson equation of state and the kinetic model developed by Vanden Bussche and Froment were selected for the VLE calculations and kinetic modeling of the reactions. All compressors including multi-stage compressors were assumed to be centrifugal compressors with isentropic efficiency of 0.75 and mechanical efficiency of 0.90. For all tube-and-shell heat exchangers, 0.1 bar and 0.5 bar pressure drops were assumed for shell- and tube-sides, respectively.

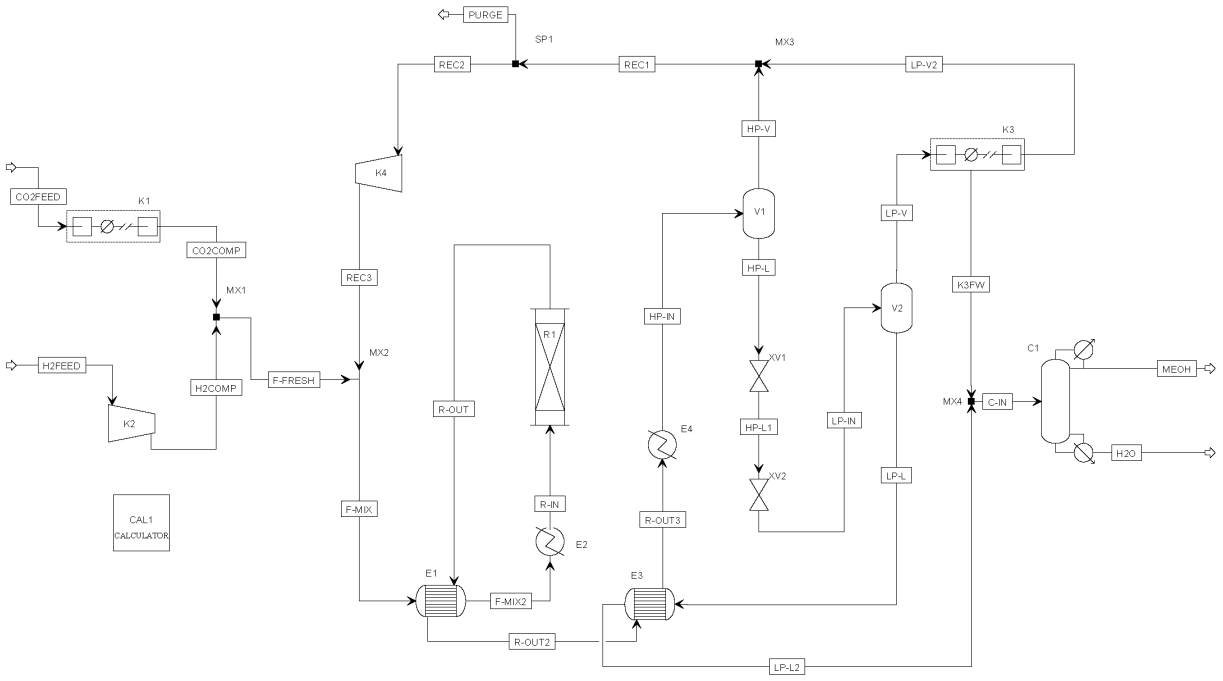

Figure 27: Proposed process for CO2 hydrogenation to MeOH.

Table 21: Assumptions for Aspen simulation implementation for carbon storage.

Assumption	**Selection/value**	**Reference**
Equation of State	Peng-Robinson	[54, 77]
Kinetic model	Vanden Bussche and Froment model	[68]
Compressor isentropic efficiency	0.75	[77]
Compressor mechanical efficiency	0.90	[78]
Shell-side pressure drop	0.1 bar	-
Tube-side pressure drop	0.5 bar	-

Vanden Bussche and Froment kinetic model was selected since it shows the best accuracy in the range of operating conditions of the reactor in this project [70]. Since Aspen Plus only accepts custom kinetic models in a designated exponential form, an algebraical rearrangement of the original model is necessary. The rate equations for methanol synthesis and reverse water-gas shift reaction in Vanden Bussche and Froment model are given in Equations 3 and 4.

$$r_{\mathrm{CH_3OH}} = \frac{k_1 P_{\mathrm{CO_2}} P_{\mathrm{H_2}} \left(1 - \frac{1}{K_{eq1}} \frac{P_{\mathrm{H_2O}} P_{\mathrm{CH_3OH}}}{P_{\mathrm{H_2}}^3 P_{\mathrm{CO_2}}}\right)}{\left(1 + k_2 \frac{P_{\mathrm{H_2O}}}{P_{\mathrm{H_2}}} + k_3 P_{\mathrm{H_2}}^{0.5} + k_4 P_{\mathrm{H_2O}}\right)^3} \tag{3}$$

$$r_{\mathrm{RWGS}} = \frac{k_5 P_{\mathrm{CO_2}} \left(1 - K_{eq2} \frac{P_{\mathrm{H_2O}} P_{\mathrm{CO}}}{P_{\mathrm{CO_2}} P_{\mathrm{H_2}}}\right)}{\left(1 + k_2 \frac{P_{\mathrm{H_2O}}}{P_{\mathrm{H_2}}} + k_3 P_{\mathrm{H_2}}^{0.5} + k_4 P_{\mathrm{H_2O}}\right)} \tag{4}$$

The kinetic parameters and equilibrium constants are given in Equations 5–7 and Table 22 [81].

$$k_i = A_i \exp \frac{B_i}{RT} \tag{5}$$

$$\log_{10} K_{eq1} = \frac{3066}{T} - 10.592 \tag{6}$$

$$\log_{10} \frac{1}{K_{eq2}} = -\frac{2073}{T} + 2.029 \tag{7}$$

Table 22: Kinetic parameters in Vanden Bussche and Froment model [B in J/mol] [81].

k_1	A_1	1.97
	B_1	40 000
k_2	A_2	3453.38
	B_2	-
k_3	A_3	0.499
	B_4	17 197
k_4	A_4	6.62×10^{-11}
	B_4	124 119
k_5	A_5	1.22×10^{10}
	B_5	−98 084

The kinetic parameters obtained after mapping them to Langmuir-Hinshelwood-Hougen-Watson (LHHW) rate expression are presented in Table 23. The pre-exponential factors and temperature exponents are set as 1 and 0, respectively, since the expression of the driving force term includes the pre-exponential term as well as the temperature dependency in the rearranged equation. The adsorption terms reported in [81] were used without any conversion.

Table 23: Coefficients for driving force constants in the kinetic model.

Reaction	**Parameter**	**CO_2 Hydrogenation**	**RWGS**
Forward	A	−29.87	4.804
	B	4811.2	−11797.5
Backward	A	17.55	0.131
	B	−2249.8	−7023.5

Table 24 presents all input specifications for the unit operation blocks used in the simulation. A packed-bed catalytic plug flow reactor (RPlug) and an equilibrium column (RadFrac) were used for the reactor and the distillation column. Compressors and heat exchangers were placed to maintain the constant reactor inlet condition at 70 bar and 220°C, flash separation pressures at 69.4 bar and 0.5 bar, and the distillation column.

Table 24: Aspen Plus input specifications for MeOH process.

Block	Specification	Input
Compressors[a]		
K1 (MCompr)	Discharge pressure	71 bar
	Number of stages	4
K2 (Compr)	Discharge pressure	71 bar
K3 (MCompr)	Discharge pressure	69.5 bar
	Number of stages	4
K4 (Compr)	Discharge pressure	71 bar
Heat exchangers		
E1 (HeatX)	Hot stream outlet temperature	150°C
E2 (Heater)	Outlet temperature	220°C
	Pressure	70 bar
	Utility	Hot oil
E3 (HeatX)	Cold stream outlet temperature	120°C
E4 (Heater)	Outlet temperature	35°C
	Pressure	69.4 bar
	Utility	Cooling water
Reactor		
R1 (RPlug)	Reactor type	Adiabatic
	Number of tubes	
	Cement	10 000
	Pulp	6 000
	Length	6 m
	Tube Diameter	0.04 m
	Pressure drop correlation	Ergun
	Catalyst bed void	0.4
	Catalyst particle density	1 775 kg/m^2
	Catalyst particle diameter	5.4 mm
Flash vessels[b]		
F1 (Flash2)	Pressure	69.4 bar
F2 (Flash2)	Pressure	0.5 bar
Distillation column		
C1 (RadFrac)	Condenser specification	Total condenser
	Number of stages	
	Cement	21
	Pulp	12
	Condenser pressure	1.5 bar
	Reflux ratio	2.5
	Bottoms rate	
	Cement	4 200 kmol/hr
	Pulp	2 900 kmol/hr

[a] The isentropic efficiency is 0.75 and the mechanical efficiency is 0.90 for all compressors.
[b] The duties are zero for all flash vessels.

Key simulation results are presented in Table 25. Although the single-pass conversion is low due to thermodynamic limitation, overall conversions exceeding 97% are achieved in both processes. This high efficiency is made possible by recycling unreacted reactants, with molar recycle ratios of 6.9 and 5.5 for the processes using captured carbon from cement and pulp plants, respectively. MeOH yields (moles of produced MeOH per mole of CO_2) are 92–94%, which aligns well with what is typically reported in the literature [60, 68–71].

Table 25: MeOH process simulation results.

Result	**Cement**	**Pulp**
Single pass conversion (%)	17.7	18.2
Overall conversion (%)	97.6	97.7
Molar recycle ratio	6.9	5.5
MeOH yield (%)	92.4	94.0
MeOH purity (wt%)	99.74	99.12

5 Economical Evaluation

This section analyzes the economic feasibility of the proposed carbon capture, storage, and utilization processes designed in Section 4. The alternatives are compared to each other by estimating a set of KPIs that indicate the economic feasibility. The main KPIs are cost per tonne captured CO_2 (CCC), net present value (NPV), and return on investment (ROI). The first of which can also be used as validation by comparing to similar studies in the literature.

5.1 Economical Methodology

The overall economic methodology is a Cost-Benefit Analysis (CBA) which aims to estimate the economic value of a project over the course of its entire lifespan. In this CBA, the overarching components are Capital Expenditure (CapEx), Operational Expenditure (OpEx), and revenue. Moreover, the CapEx is annualized with an interest rate to pay it off over the projects lifespan, rather than being a one-time expense. In this way, all components can be combined for each year of the project lifespan, having adjusted for different annual growth of prices and discount rates, resulting in an estimated NPV.

Net present value (NPV) is a financial measure used to look into the profitability of an investment or project by determining the difference between the present value of expected cash inflows and the present value of projected cash outflows over a specified time period. This metric offers essential insights into the economic feasibility and potential returns of CCUS, and evaluates its overall financial viability.

Return on investment (ROI) is a financial metric used to calculate the efficiency of a venture to generate profit relative to the investment. By dividing the NPV with the total investment, the generated revenue surplus as a percentage of the investment is determined. The formula for ROI is found in Equation 8.

$$\text{ROI} = \frac{\text{NPV}}{\text{Investment Cost}} \times 100\% \tag{8}$$

Once all the KPIs have been estimated, a sensitivity analysis is conducted to give insight into which inputs are the strongest influence on the ROI. The overall economic methodology is summarized in Figure 28.

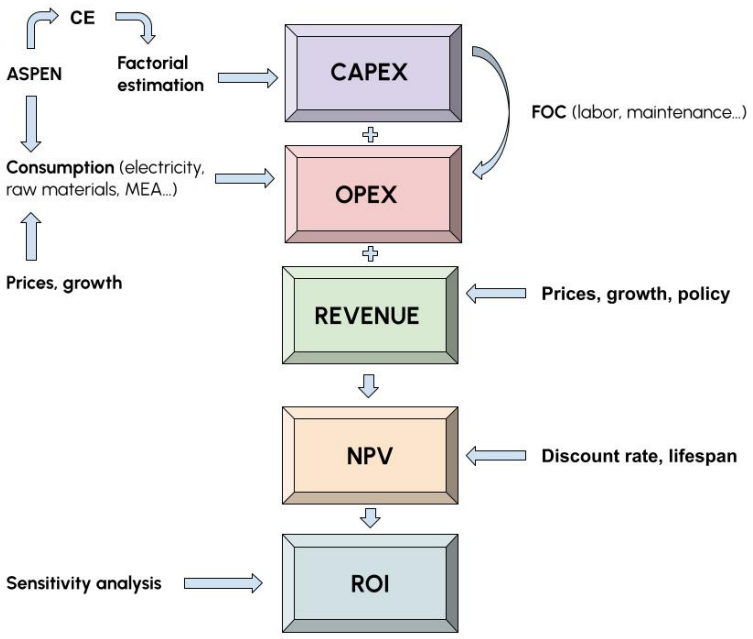

Figure 28: Splits of constituents for the VOC.

In the following sections, each major component of the CBA is explored, detailing their constituents and how they are estimated.

5.1.1 Cost Conversions

All costs in this analysis are presented in Swedish Krona (SEK) in the year 2023. The costs are adjusted for inflation with the Chemical Engineering Plant Cost Index (CEPCI) formula in Equation 9

$$C_{2023} = C_{ref} \times \frac{CEPCI_{2023}}{CEPCI_{ref}} \tag{9}$$

where C represents the cost and $CEPCI$ is the chemical engineering plant cost index [82]. For costs in other currencies, they are converted to SEK with the average exchange rate for 2023. Some important conversions are 10.61284 SEK/USD and 11.47652 SEK/EUR [83].

5.1.2 Cost Data Collection

The economic analysis for the CCUS process was achieved using a combination of modeling tools and data sources. The equipment and installation costs were primarily obtained from the Aspen Process Economic Analysis (APEA) tool. The equipment costs (Ce) which could not be determined in Aspen, were determined from literature, industrial reports, or from correlations such as the six-tenths rule. Operating expenses and revenue streams were similarly determined with Aspen for utility and raw material demands, and supplemented with their unit costs from literature and industrial reports.

To account for the cost and revenue variation over time, growth and inflation rates were also incorporated into the analysis. The growth rate refers to the annual percentage change in a cost or revenue which reflects factors such as technological advancements and market demands. Additionally, to get a more accurate cost estimation the average inflation rate for Sweden was incorporated into the cost. With the inflation rate and the growth rate of each unit, a more robust framework and understanding of the cost trend can be established, resulting in a more reliable and accurate analysis.

5.2 Capital Expenditure

Capital expenditures (CapEx) for CCUS represents the upfront investment required to design, construct, and implement infrastructure for capturing, transporting, and converting CO_2 into valuable products, or sequestration. CapEx is primarily estimated using the factorial method, a percentage-based formula of equipment costs (Ce) in the core process design [84].

5.2.1 Equipment Purchase Costs

The equipment costs are primarily obtained from the Aspen Process Economic Analysis (APEA) tool as summarized in Table 26. Each of the unit operation blocks in the simulations were mapped to a corresponding APEA model and dimensioned using their sizing equations.

Table 26: Equipment cost for proposed CCUS process in M SEK$_{2023}$.

Process	Equipment Type	Cement	Pulp
Capture	Absorber	228.0	179.1
	Stripper	570.1	494.8
	Heat exchanger	36.0	4.4
	Coolers	9.0	21.7
	Flash drums	2.9	1.3
	Pumps	3.3	2.7
Utilization	Distillation column	33.9	21.2
	Heat exchangers	59.0	37.1
	Compressors	491.9	408.9
	Reactor[a]	20.7	16.9
	Flash vessels	8.1	5.7
Storage	Compressors	295.3	225.3
	Coolers	8.0	6.5
	Heat exchanger	10.8	5.0
	Flash vessels	2.5	2.0
	Temporary storage tank[b]	225.0	225.0
Capture and Utilization		**1 462.8**	**1 193.8**
Capture and Storage		**1 390.9**	**1 167.9**

[a] Reactor cost determined by six-tenths rule (Section 5.2.2).
[b] Temporary storage tank cost determined from [80].

The equipment cost for the capture and storage process is compared to the cost found in literature [85] and scaled using the six-tenths method described in Section 5.2.2 based on the amount of CO_2 captured. The resulting costs were found to be of the same order of magnitude and within 30% which indicates that the Aspen data is sufficiently accurate for this phase of the study.

5.2.2 Equipment Purchase Cost Estimation by Six-tenths Rule

The six-tenths rule is a widely used method in engineering economics to estimate the cost of industrial equipment based on scaling based on reference equipment [84]. Since the cost for the reactor for the methanol synthesis could not be determined in APEA, likely due to the tube thickness calculation, the six-tenths rule was used to scale the cost of a reference reactor of similar conditions to the scale of the proposed process reactor using the correlation in Equation 10.

$$C = C_{\text{ref}} \times \left(\frac{Q}{Q_{\text{ref}}} \right)^n \tag{10}$$

C is the reactor cost of the process to be estimated, C_{ref} is the known reference cost of equipment from literature, Q is the capacity of the equipment in the process, and Q_{ref} the reference process equipment capacity. The scaling exponent n is based on empirical data for equipment geometries. In this case, $n = 0.6$[84]. The reactor cost using the sixth-tenths rule for cement and pulp in the methanol production can be seen in Table 26.

5.2.3 CapEx Estimation

CapEx is estimated using the factorial method described by Sinott & Towler [84]. The main function of this method is to use equipment costs for the process as inputs and estimate all additional associated CapEx using percentage-based factors from empirical data within the industry. The on-site costs include constituents such as piping, equipment erection, and instrumentation, while other costs include off-sites, design & engineering, and contingencies. Equation 11 shows the formula for the factorial estimation. Tables 27-28 contain the CapEx factors for each plant based on a factor of the equipment costs. The CapEx for each unit in the process is calculated from the equipment purchase cost as follows:

$$\text{CapEx} = \sum C_e \times (1 + f_p + f_{\text{er}} + f_{ic} + f_{\text{el}} + f_{\text{c}} + f_{\text{sb}} + f_{\text{lp}}) \times (1 + f_{os}) \times (1 + f_{\text{de}} + f_{\text{co}}) \tag{11}$$

Table 27: CapEx Estimation for CCUS for cement plant in M SEK$_{2023}$.

Constituent	Factor	Utilization	Storage
Piping (f_p)	0.80	1 170.2	1 112.7
Equipment erection (f_{er})	0.30	438.8	417.3
Instrumentation & control (f_{ic})	0.30	438.8	417.3
Electrical (f_{el})	0.20	292.6	278.2
Civil (f_c)	0.30	438.8	417.3
Structures & buildings (f_{sb})	0.20	292.6	278.2
Lagging & paint (f_{lp})	0.10	146.3	139.1
Total onsite capital costs	**3.20**	**4 681.0**	**4 451.0**
Off sites (f_{os})	0.30	438.8	417.3
Design & engineering (f_{de})	0.30	438.8	417.3
Contingencies (f_{co})	0.10	146.3	139.1
Total CapEx	**5.82**	**8 519.4**	**8 100.8**

Table 28: CapEx Estimation for CCUS for pulp plant in M SEK$_{2023}$.

Constituent	Factor	Utilization	Storage
Piping (f_p)	0.80	955.0	934.3
Equipment erection (f_{er})	0.30	358.1	350.3
Instrumentation & control (f_{ic})	0.30	358.1	350.3
Electrical (f_{el})	0.20	238.7	233.5
Civil (f_c)	0.30	358.1	350.3
Structures & buildings (f_{sb})	0.20	238.7	233.5
Lagging & paint (f_{lp})	0.10	119.3	116.7
Total onsite capital costs	**3.20**	**3 820.2**	**3 737.2**
Offsites (f_{os})	0.30	358.1	350.3
Design & engineering (f_{de})	0.30	358.1	350.3
Contingencies (f_{co})	0.10	119.3	116.7
Total CapEx	**5.82**	**6 952.7**	**6 801.8**

5.2.4 Annualized Capital Cost

To more accurately calculate the total capture cost of the CCUS process, the total CapEx is annualized into the Equivalent Annual Cost (EAC). This transformation distributes the one-time upfront investment evenly over the lifespan of the equipment and accounts for the time value of money. Additionally, it enables a better comparison between the CapEx and OpEx contributions to the total costs. The equivalent annual cost is calculated as follows [86]:

$$\text{EAC} = \frac{\text{CapEx}}{A} \tag{12}$$

where A is the annualization factor which is calculated as follows:

$$A = \frac{1 - \frac{1}{(1+r)^t}}{r} \tag{13}$$

where r is the economic depreciation and t is the total project lifespan.

5.3 Operating Expenditure

Operational Expenditure (OpEx) refers to the ongoing costs associated with operating and maintaining each process. The OpEx are classified into variable operational costs (VOC) and fixed operational costs (FOC). VOC includes the costs that depend on the system's capacity and production which includes the expenses for consumables such as raw materials and utilities. FOC remains relatively constant regardless of the system's capacity and includes factors such as taxes, labor, administration, and maintenance. The reason for this being that FOC is estimated based on a relationship between CapEx and OpEx, where CapEx is the most heavily influencing factor. This is explained in further detail in section 5.3.2.

5.3.1 Market Prices of Consumables

The main consumables in the CCUS processes are hydrogen, monoethanolamine (MEA), and electricity. Hydrogen is the feedstock for the methanol synthesis process. MEA is the solvent used to capture CO_2 and a small fraction is consistently purged and replenished to avoid a build-up of impurities and degradation. Electricity is required to power equipment such as compressors and pumps and in order to generate steam. To ensure the process does not contribute to additional carbon emissions, the electricity and hydrogen must be from green, renewable resources. The costs and projected growth for the process consumables are summarized in Table 29 below.

Table 29: Utility and raw material costs.

Material or Utility	Purpose	Cost	Growth	Reference
Green hydrogen	Feedstock	71 880 SEK/t-H_2	0.615%	[87]
MEA	Solvent	8 597.78 SEK/t-MEA	0.575%	[88]
Renewable electricity	Energy source	0.28 SEK/kWh	0.615%	[89]

The current costs and projected growth rates of utilities and raw materials were in turn supplemented with the annual demand for those consumables based on Aspen simulations. This way, annual costs could be calculated.

5.3.2 Estimating Fixed Operational Costs

The fixed operational costs (FOC) were estimated from factors of the CapEx and OpEx based on Sinott & Towler [84, 90]. The OpEx and the FOC are calculated simultaneously from Equation 14, which depends on the factors in Tables 30 to 31.

$$\text{OpEx} = \text{VOC} + \text{FOC} = \frac{\text{VOC} + 0.05 \times \text{CapEx}}{1 - 0.155} \tag{14}$$

Table 30: Fixed operational costs for cement plant in M SEK_{2023}.

Cost type	CapEx Factor	OpEx Factor	Utilization	Storage
Local tax	0.01	-	85.2	122.4
Insurance	0.01	-	85.2	122.4
Maintenance	0.03	-	255.8	376.2
Operating labor	-	0.1	1 499.4	130.6
Distribution	-	0.005	74.9	6.5
R&D costs	-	0.05	749.7	65.3
Total			**2 750.07**	**814.5**

Table 31: Fixed operational costs for pulp plant in M SEK_{2023}.

Cost type	CapEx Factor	OpEx Factor	Utilization	Storage
Local tax	0.01	-	69.5	109.4
Insurance	0.01	-	69.5	109.4
Maintenance	0.03	-	208.6	328.2
Operating labor	-	0.1	1 129.5	108.2
Distribution	-	0.005	56.5	5.4
R&D costs	-	0.05	564.7	54.1
Total FOC			**2 098.2**	**714.8**

5.4 Revenue

Revenue from CCS and CCU, specifically methanol production and carbon storage, depends on the type of carbon, market demand, government incentives, and carbon pricing [91]. Carbon is priced in Sweden either through carbon tax or EU ETS [92]. The EU ETS or the European Emissions Trading System is a carbon market that aims to reduce emissions in the EU by setting a cap on total emissions, that requires companies to purchase allowances for their emissions. It covers sectors like electricity generation, heavy industry, and aviation [93]. Fossil-based emissions increase the total carbon in the atmosphere, contributing to climate change. On the other hand, biogenic emissions originate from carbon already within the natural carbon cycle and are considered carbon-neutral. Consequently, only fossil carbon emissions are accounted for in the EU ETS, which means only the cement plant falls under its scope [93].

Table 32: Potential revenue sources for CCUS.

Case No.	Feed Type	Carbon Application	Revenue Source
1	Cement	Utilization	MeOH sales
2	Cement	Storage	ETS (fossil)
3	Pulp	Utilization	MeOH sales
4	Pulp	Storage	N/A

5.4.1 Methanol Production vs Storage

CCS can help cement producers reduce costs under the EU ETS. By capturing and storing CO_2, producers lower their reportable emissions, meaning they need to buy fewer allowances. If they have already purchased allowances, the captured CO_2 creates a surplus, allowing them to sell the unused allowances on the carbon market. With carbon prices currently at 778.80 SEK/t-CO_2 (see Table 33), this ability to reduce purchases or sell surplus allowances provides a strong financial incentive to invest in CCS [94].

CO_2 capture from pulp mills is feasible with the right policies. However, the EU ETS currently treats captured and stored biogenic CO_2 as carbon neutral rather than carbon negative. Introducing incentives for negative emissions is crucial to drive CCS adoption, enabling the industry to offset costs and generate new revenue opportunities [95].

Methanol production offers revenue opportunities for CCU projects. Instead of simply storing captured CO_2, converting it into methanol creates a valuable commodity with diverse market applications. The current market price for methanol can be seen in Table 33.

Table 33: Summary of Revenue Sources, Unit Revenues, and Growth Rates.

Revenue sources	Unit revenue	Annual growth	Reference
Credits [SEK/t-CO_2]	778.80	7.90%	[96, 97]
MeOH sales [SEK/t-MeOH]	3 760.77	1.43%	[98, 99]

The outputs of MeOH and stored fossil CO_2 were extracted from each process to supplement the current annual prices and annual growth. This way, annual revenue could be calculated.

5.5 Discounting

The discount rate is crucial in evaluating environmental projects as it determines the present value of future costs and benefits. Traditional financial discount rates are often too high for long-term environmental investments, such as climate change mitigation, as they undervalue the importance of future benefits. Instead, a social discount rate, which is typically lower than financial rates is recommended. This approach values future and current generations equally, encouraging more investment in sustainability. By integrating social capital into decision-making through lower discount rates, companies, and policymakers can better ad-

dress long-term environmental challenges [100].

For CCUS projects, the choice of discount rate becomes especially important because these initiatives are long-term, and their primary benefits such as reduced greenhouse gas emissions and mitigated climate change span over decades. A lower discount rate of 1–3% is often used for such projects as it represents the long-term value of environmental benefits for future generations. Therefore, in this economic analysis, a discount rate of 3% will be used [101].

5.6 Project lifespan

The project life span refers to the whole duration of our project, it encompasses all the phases for our project to achieve its objectives. The lifespan of 25 years was determined by looking at another project with a similar design and processes [60].

5.7 Sensitivity Analysis

A sensitivity analysis is crucial to forecast how changes in different variables will affect the profitability of the designed system. Two sensitivity analyses were conducted; one for the highest ROI score for storage, and one for the highest ROI score of utilization, those being cement-storage and pulp-utilization. In each sensitivity analysis, a set of inputs deemed most relevant for the ROI score were set to a lower bound, baseline, and upper bound. It was then analyzed how the changes in input value would impact the ROI.

It is important to note that the lower and upper bounds for each input were selected based on a reasonable range in which they may realistically vary. The only absolute cost included is the total equipment cost (Ce). This input was varied by ±30% which is directly linked to the margin of error of a study estimate, which is the level of economic estimation that has been applied during this project. This margin accounts for potential inaccuracies in APEA to conduct of costing. As other absolute values such as prices of goods and utilities were found in the literature with relative certainty, all remaining inputs were based on uncertain factors, such as growth rates of prices, wages, and discount rate. Since these inputs are already based on annual percentages, the range of variation was set to ±2%.

6 Results & Discussions

6.1 Technical

The overall CCUS process for two industrial effluent streams is shown in Figure 29 below.

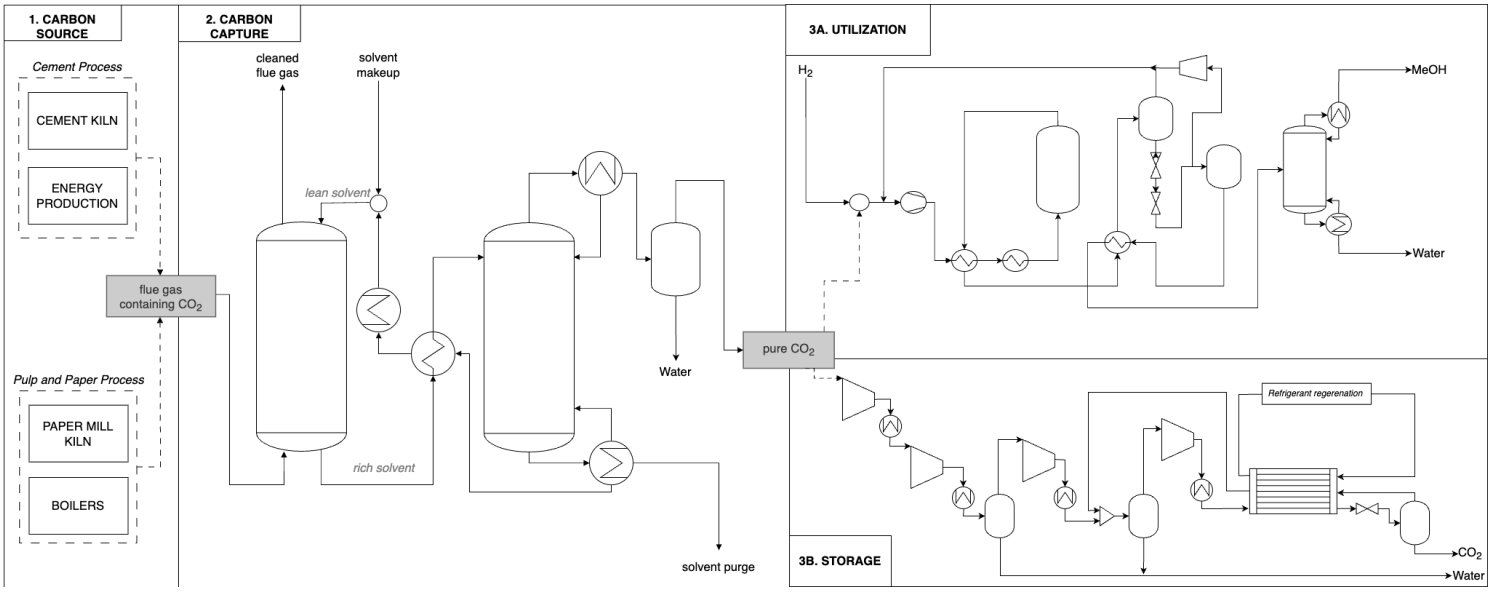

Figure 29: Process Flow Diagram for overall proposed CCUS.

The model for carbon capture was primarily modeled to be as efficient in its ability to remove CO_2 as possible. How feasible the design process was in regards to energy usage was not taken into consideration. This caused a higher than average capture rate at the cost of increased energy usage. This is in large part due to the reboil ratio being as high as it is at 0.9. The results in an energy per t-CO_2 captured to be 27.02 GJ/t-CO_2. This is about 3 times as much compared to other studies on the subject [73]. However, our proposed system uses less MEA than the same study. The proposed model uses about 1.7 tonnes of solvent per tonne CO_2 capture while the compared system uses 3.33 tonne MEA per tonne CO_2 captured. The reason for reducing the amount of solvent used instead of decreasing the energy usage is in large part to decrease the size of the absorber and stripper.

6.2 Economical

6.2.1 Key Performance Indicators

Key Performance Indicators (KPIs) are metrics used to assess the proposed process results. Three critical KPIs are the cost of carbon capture (CCC), net present value (NPV), and return on investment (ROI), which can be seen in Table 34.

Table 34: KPIs for all scenarios considered.

Plant Type	**Cement**		**Pulp**	
Application	**Utilization**	**Storage**	**Utilization**	**Storage**
CCC (SEK/t-CO_2)	10 800	1 895	10 700	2 130
NPV (M SEK_{2023})	−140 100	−19 200	−105 500	−50 000
ROI (%)	−64.3	−28.3	−64.1	−99.1

The NPV over the project lifespan is shown in Figure 30. Of the four scenarios considered, none reach an NPV of zero and therefore none of the proposed projects are financially viable for the current conditions.

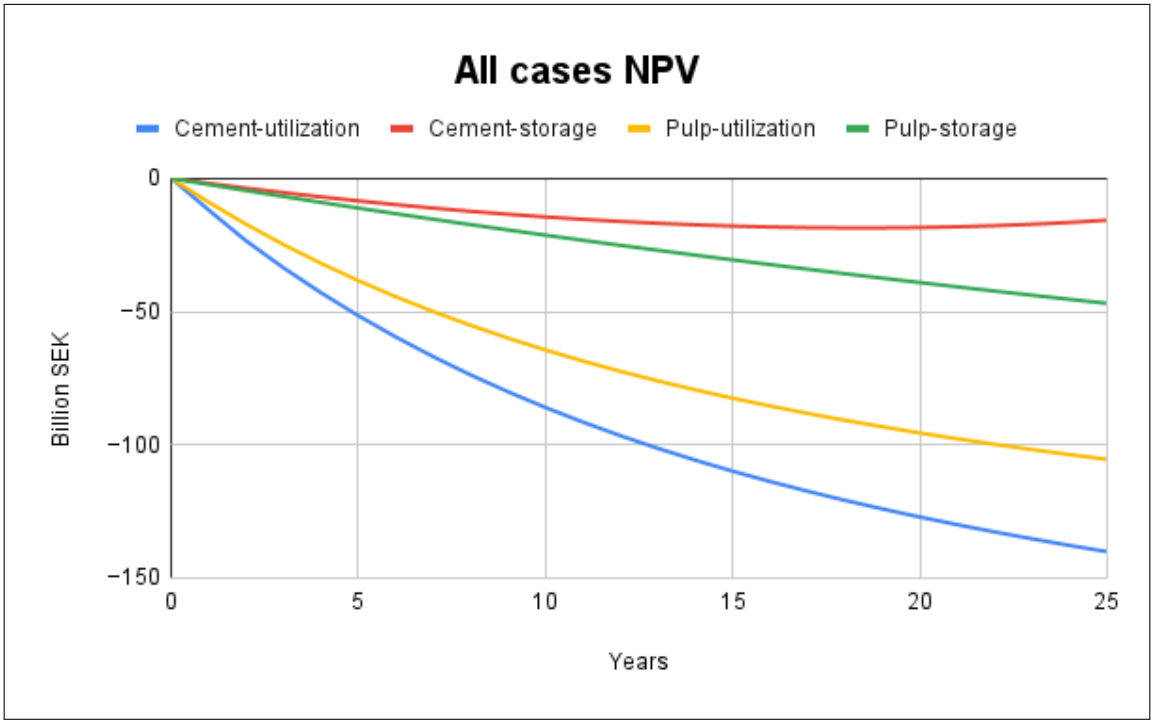

Figure 30: NPV over course of project lifespan.

The contributions to the NPV of the CapEx, Variable operational costs, and fixed operational costs at the end of the project lifespan are shown in Figure 31 below.

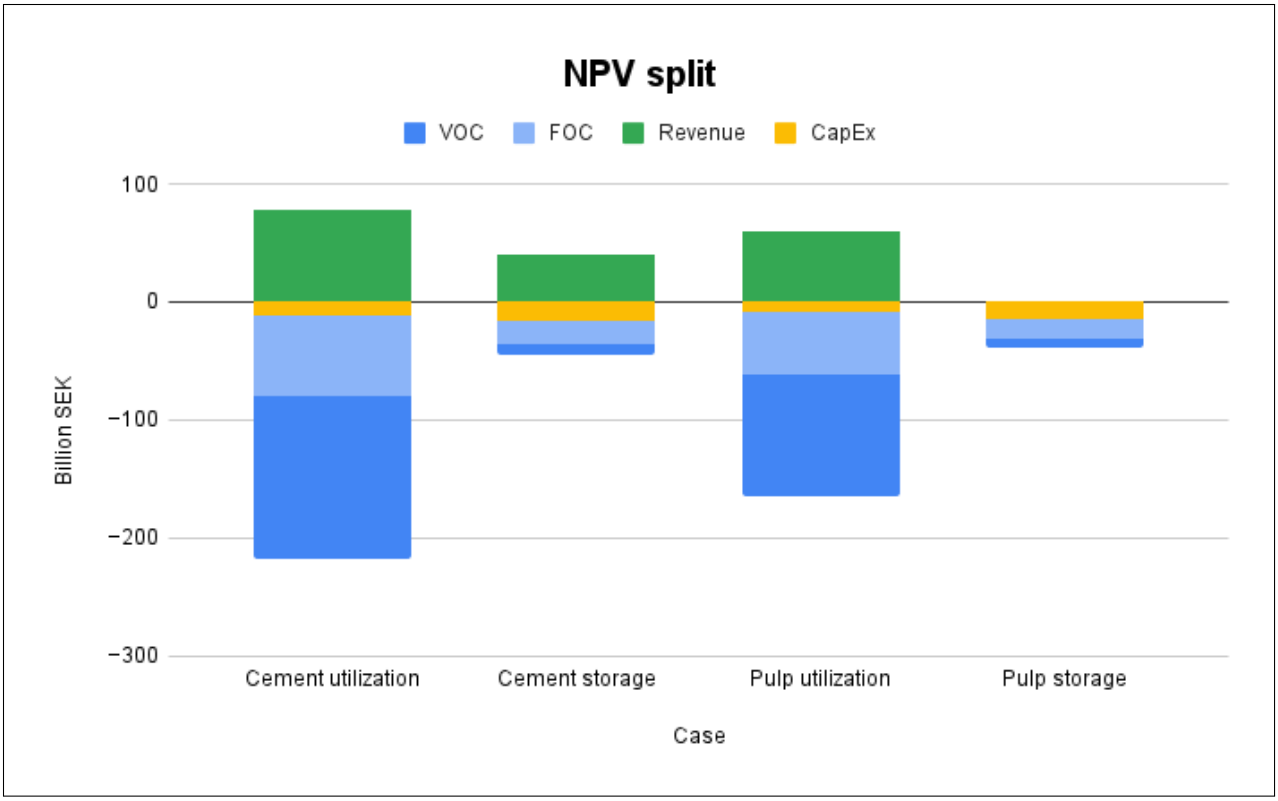

Figure 31: Splits of constituents for the NPV.

Figure 31 shows that the cases with utilization have high total OpEx over the lifespan of the project, both in FOC and VOC in relation to CapEx and revenue. Due to the lower flue gas flow rate in the pulp plant, the magnitude of all NPV constituents is smaller than for the cement plant. A similar observation can be made about the storage cases, except with higher relative CapEx instead of OpEx. One noticeable difference though is how the pulp plant does not generate revenue from carbon credits, reflecting what was discussed earlier.

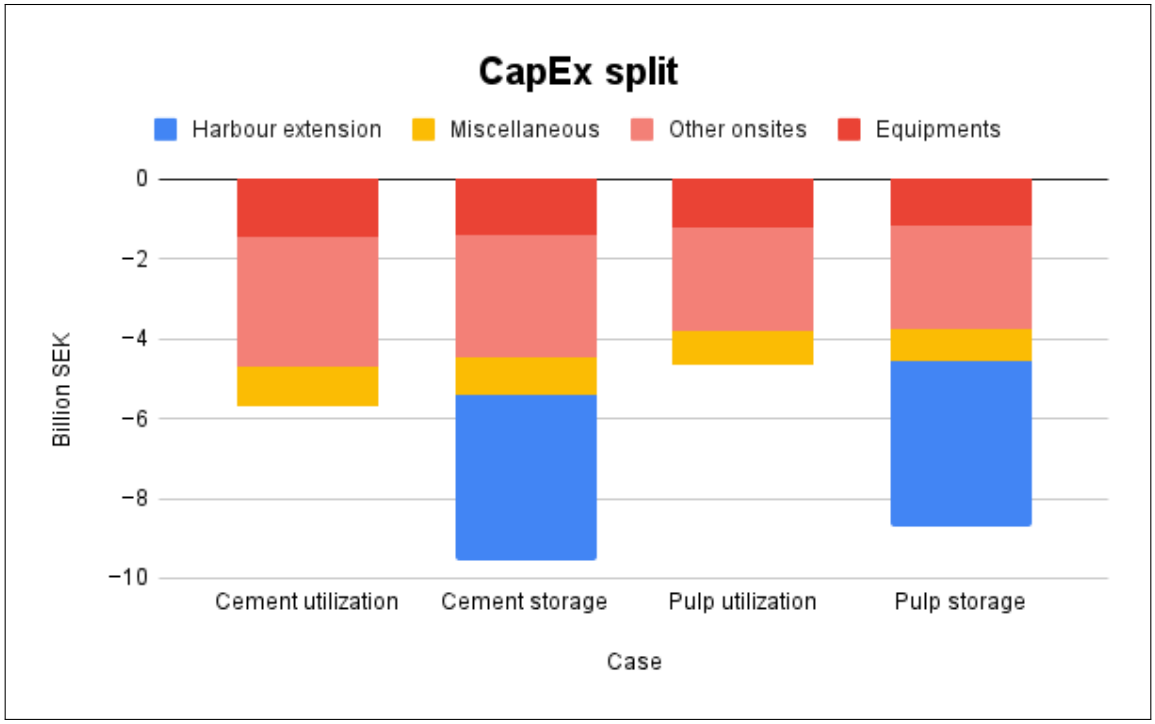

Figure 32: Splits of constituents for the CapEx.

As can be seen in Figure 32, onsite costs remain high contributors to the total CapEx across all cases, with equipment cost being the largest. Other onsite costs include additional supporting infrastructure such as piping, instrumentation, and buildings. The smallest contributor to the CapEx is miscellaneous which includes costs such as offsites and contingencies. The proportionality of equipment costs (Ce), other onsites, and miscellaneous remains the same across all four cases. This is due to them all being estimated using the factorial method. However, for the storage alternatives, the required harbor extension leads to a considerable cost as well.

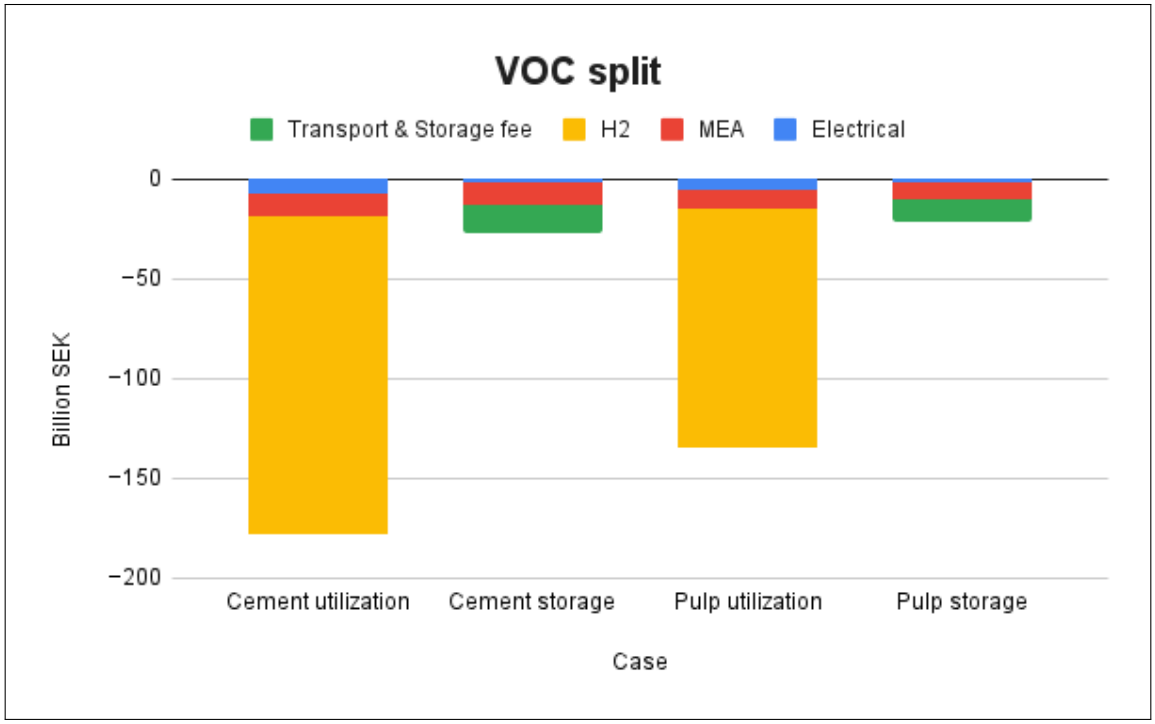

Figure 33: Splits of constituents for the VOC.

Figure 33 highlights the significant cost of green H_2 in utilization scenarios for both cement and pulp. The other VOCs, such as MEA and electrical costs, also contribute to the VOC but to a much smaller extent. For CCS options, the storage and transportation fee from Northern Lights for the storage options is much cheaper in contrast to that of green H_2.

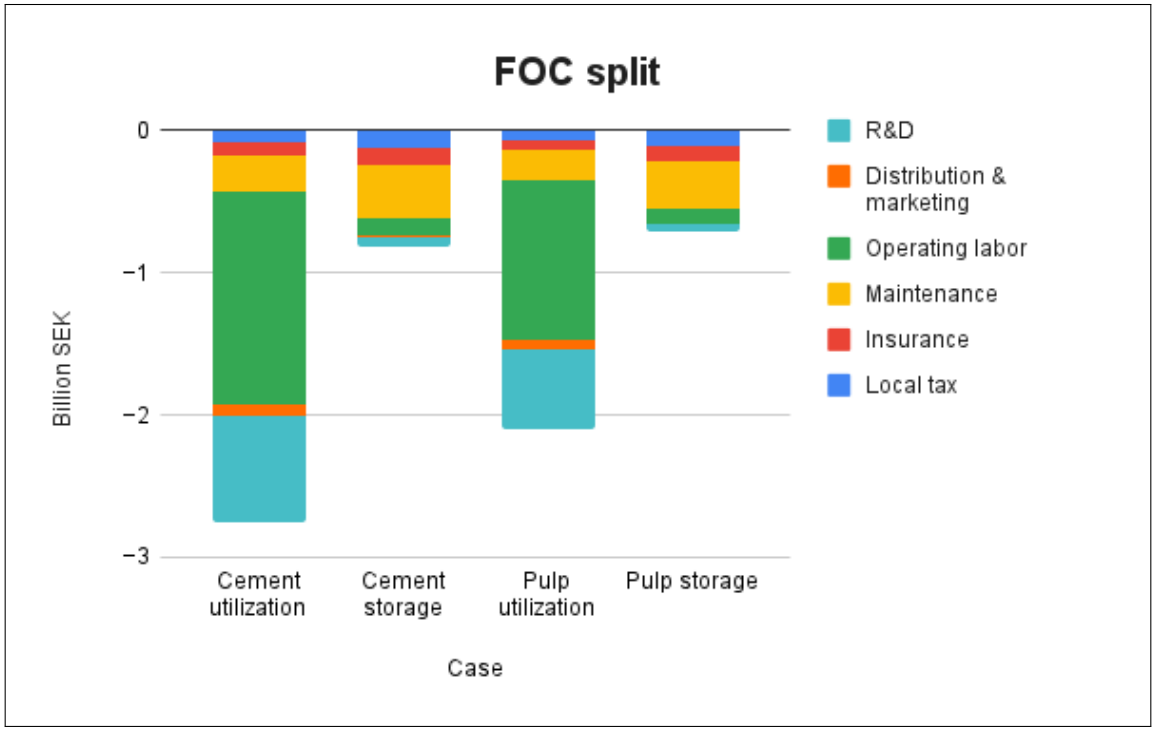

Figure 34: Splits of constituents for the FOC.

Figure 34 showcases the FOC constituents for each case. Since FOC is an estimation where both CapEx and VOC are inputs, and these vary between each case, the FOC constituents relative contribution to the total differs. For utilization cases, the elevated VOCs cause higher operating labor, distribution, marketing, and R&D. In contrast, storage cases with higher CapEx due to the harbor extension have raised local tax, insurance, and maintenance instead.

6.2.2 Sensitivity Analysis

The results of the sensitivity analysis performed can be interpreted as a profitability map for the investment in the proposed CCUS processes. As all ROIs of this project are estimated to be negative, it is important to note that Figures 35 to 36 show the percent change in negative ROI.

In practical terms, it means that negative ROI decreases downward along the y-axis. As an example, a point being closer to the x-axis would therefore represent a change in the positive direction for the ROI and should be interpreted as being less unprofitable.

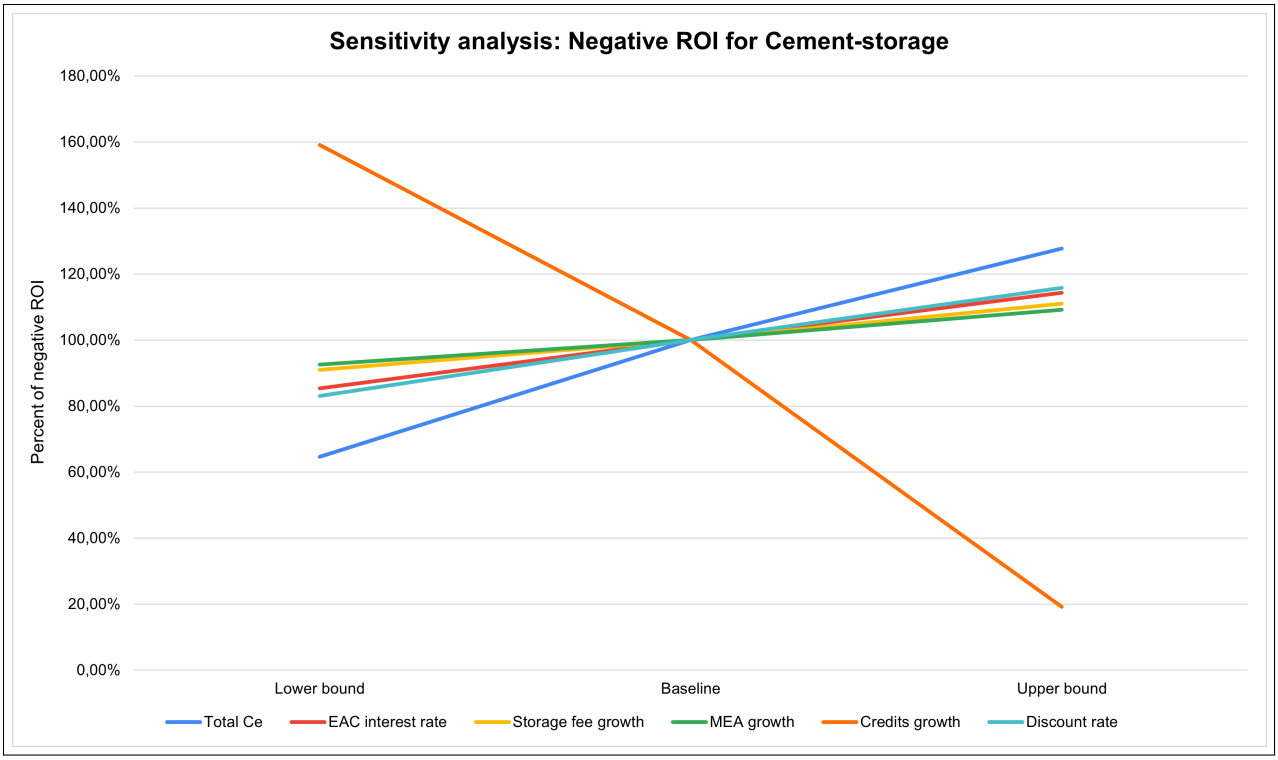

Figure 35: Negative ROI sensitivity analysis for cement CCS. All % based inputs varied by ± 2%, Ce varied by ± 30%.

For cement storage in Figure 35, it is immediately evident that the growth of credits has a high impact on the ROI, with the lower bound reaching around 160% of the negative ROI while the upper bound reaches approximately 20%. This is due to carbon credits being the only revenue source of the project, combined with the fact that this is the least unprofitable alternative. Had the total revenue been less, a change in credit growth would not have made as much of a difference in the ROI. See figure 31 for further insight. This is an especially interesting observation, as the annual growth of carbon credits is a highly discussed and uncertain topic. This indicates a slight possibility of economic viability for retrofitting CCS technology to the cement plant in Slite, especially when reducing costs elsewhere. This can be achieved by increasing economic efficiency in the CC process by sacrificing the upper percentages of CC efficiency or choosing pipeline as mode of transportation instead of shipping which also has a smaller requirement of compression.

The same principle of relative contribution to the NPV applies to another input of note; Total Ce. This is the main contributor to CapEx through the factorial estimation, and CapEx is the second most significant contributor to the NPV of the cement-storage alternative. All other input parameters were likewise chosen for their deemed high impact on the ROI. Even so, the annual growth of credits remains the by far most contributing factor.

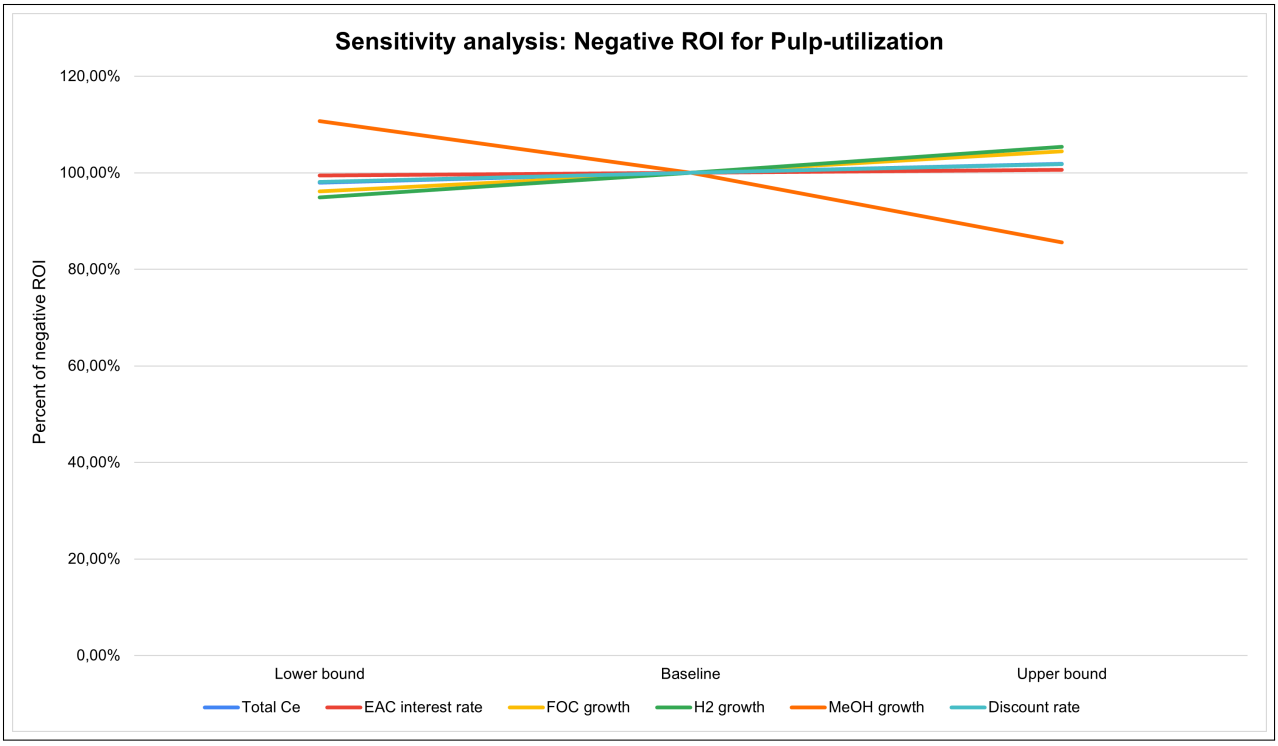

Figure 36: Negative ROI sensitivity analysis for pulp CCU. All % based inputs varied by ± 2%, Ce varied by ± 30%.

For pulp-utilization in Figure 36, the sensitivity is much more equally distributed across the selected inputs. Again, this case only has one source of revenue, likely explaining why the highest sensitivity is attributed to the MeOH price growth input. However, the relative sensitivity is much less pronounced in this case. This occurs because the high fixed and variable operating costs outweigh the revenue to a further extent, resulting in smaller contributions to the ROI from revenue. Similarly, since CapEx is a much smaller contributor to the NPV in this case, total Ce and EAC interest rate are rendered much less detrimental to the ROI as well. In contrast, VOC and FOC are the main contributors, with H_2 being the by far most contributing component of VOC. This is also reflected in Figures 35-36. To summarize, the factors most influencing the ROI of the pulp-utilization alternative are the price inflations of MeOH and, to a lesser extent, H_2.

Lastly, when comparing Figures 35-36 overall, it is clear that cement-storage seems generally more sensitive regardless of input, as the bounds are further apart and spread across a larger percentage-based impact. For Pulp-utilization on the other hand, the opposite is observed. This is accredited to the fact that the negative NPV of the pulp-utilization is nearly twice that of cement-storage, and that changes of input values will be less impactful when observing on a percentage-based scale.

7 Conclusion

Carbon Capture Utilization and Storage is an option for Swedish industries to reduce CO_2 emissions. Carbon capture utilization (CCU) and carbon capture storage (CCS) have distinct motivations: CCU promotes a circular economy whereas CCS enables a permanent sequestration for CO_2. This techno-economic investigation analyzes the economic feasibility of these approaches retrofitted to two key industrial processes: cement production, which primarily emits fossil-based CO_2, and pulp production, which emits biogenic CO_2. Under the current conditions, none of the proposed processes for the four scenarios considered are economically viable to capture CO_2, regardless of the downstream application.

7.1 Utilization

The proposed CCU process is not economically feasible under the current conditions for cement or pulp plants. The primary reasons the process is not competitive with conventional, fossil-based processes are due to the high cost of green hydrogen. The current market price of methanol is 3 760.77 SEK/t [98], while the levelized cost of methanol produced in the proposed process (LCOM) is 13 975.00 SEK/t, nearly 4 times higher. The sensitivity analyses revealed the profitability of the process is highly sensitive to the cost of feed hydrogen. If the green hydrogen price reaches 12 000 SEK/t, approximately one-fifth of the current price in Sweden, the LCOM from the proposed process will be competitive in the market without any subsidies.

Therefore, while CCU, specifically in the form of hydrogenation into methanol, has the potential to repurpose CO_2 and enable a circular economy, achieving economic feasibility requires advancements in technology, reductions in green hydrogen costs, and robust incentives to enable market competitiveness with fossil-derived methanol.

7.2 Storage

The proposed CCS process is not economically feasible for cement or pulp plants under the current conditions. The cost per tonne of CO_2 of the proposed process is approximately twice as expensive as in literature due to the added complexities associated with shipping, such as the liquefaction process, harbor extension, and shipping company cost. This is because no viable carbon storage locations are accessible by pipeline in Sweden [32, 34].

The proposed CCS process could become more economically feasible with more favorable policy interventions, such as higher carbon credit growth rates and the inclusion of biogenic emissions in carbon trading frameworks. Under the current conditions, however, the EU Emissions Trading System only considers fossil CO_2, covering 88% of cement and barely 1% of pulp emissions in this study. For the CCS process for the cement plant to break even, the EU ETS carbon credit price would need to grow by 10.3% annually, which is roughly double the current projected growth. This highlights the need for stronger policy support for CCS. While incentives for capturing and storing fossil CO_2 are important to decrease industrial emissions, true net zero is unlikely since certain sectors will continue to emit CO_2. There-

fore, incentives for both biogenic and fossil credits within the EU ETS, with a growth rate of about 9.5%, would generate enough revenue for both the cement and pulp plants considered to break even within the plant lifespan. This approach would enable negative emissions from biogenic carbon, thereby helping to reach net zero by offsetting emissions from sectors that face challenges in decarbonization.

References

[1] Song Nie et al. "Analysis of theoretical carbon dioxide emissions from cement production: Methodology and application". In: *Journal of Cleaner Production* 334 (Feb. 2022), p. 130270. ISSN: 0959-6526. DOI: 10.1016/j.jclepro.2021.130270. URL: https://www.sciencedirect.com/science/article/pii/S0959652621044358 (visited on 11/13/2024).

[2] OAR US EPA. *Carbon Dioxide Emissions Associated with Bioenergy and Other Biogenic Sources*. en. Overviews and Factsheets. URL: https://19january2017snapshot.epa.gov/climatechange/carbon-dioxide-emissions-associated-bioenergy-and-other-biogenic-sources (visited on 11/13/2024).

[3] *Ministry of Energy and Energy Industries — Carbon Capture Utilization and Storage (CCUS)*. URL: https://www.energy.gov.tt/our-business/carbon-capture-utilization-and-storage-ccus/ (visited on 11/26/2024).

[4] Matt. *Understanding Carbon Capture Use Storage (CCUS)*. en-GB. Dec. 2021. URL: https://ccushub.ogci.com/ccus-basics/understanding-ccus/ (visited on 11/15/2024).

[5] Tom Mikunda et al. "Carbon capture and storage and the sustainable development goals". In: *International Journal of Greenhouse Gas Control* 108 (June 2021), p. 103318. ISSN: 1750-5836. DOI: 10.1016/j.ijggc.2021.103318. URL: https://www.sciencedirect.com/science/article/pii/S1750583621000700 (visited on 11/13/2024).

[6] Barbara Olfe-Kräutlein. "Advancing CCU Technologies Pursuant to the SDGs: A Challenge for Policy Making". English. In: *Frontiers in Energy Research* 8 (Aug. 2020). Publisher: Frontiers. ISSN: 2296-598X. DOI: 10.3389/fenrg.2020.00198. URL: https://www.frontiersin.org/journals/energy-research/articles/10.3389/fenrg.2020.00198/full (visited on 11/13/2024).

[7] *Fossil vs biogenic CO2 emissions – Bioenergy*. en-US. URL: https://www.ieabioenergy.com/iea-publications/faq/woodybiomass/biogenic-co2/ (visited on 11/14/2024).

[8] *Cementproduktion steg-för-steg — Heidelberg Materials Cement Sverige*. sv. URL: https://www.cement.heidelbergmaterials.se/sv/cementproduktion-steg-f%C3%B6r-steg (visited on 11/26/2024).

[9] *Cement industry*. en-GB. URL: https://fossilfrittsverige.se/en/roadmap/the-cement-industry/ (visited on 11/13/2024).

[10] Mariel Vilella and Carlos Arribas. "Report prepared for the European Commission in the framework of the reform of the EU Emissions Trading Scheme (EU ETS)". en. In: ().

[11] *Anläggningssida*. URL: https://utslappisiffror.naturvardsverket.se/sv/Sok/Anlaggningssida/?pid=200 (visited on 11/26/2024).

[12] *Table 2 Cement plant flue gas characteristics.* en. URL: https://www.researchgate.net/figure/Cement-plant-flue-gas-characteristics_tbl2_321760809 (visited on 11/26/2024).

[13] Mónica P. S. Santos, Vasilije Manovic, and Dawid P. Hanak. "Unlocking the potential of pulp and paper industry to achieve carbon-negative emissions via calcium looping retrofit". In: *Journal of Cleaner Production* 280 (Jan. 2021), p. 124431. ISSN: 0959-6526. DOI: 10.1016/j.jclepro.2020.124431. URL: https://www.sciencedirect.com/science/article/pii/S0959652620344759 (visited on 11/26/2024).

[14] *Gävle bruk*. sv. URL: https://www.billerud.se/om-billerud/vara-produktionsanlaggningar/gavle (visited on 11/26/2024).

[15] "(PDF) The Influence of Lignin Removal on the Energy Balance of Future Pulp Mills". en. In: *ResearchGate*. URL: https://www.researchgate.net/publication/272499660_The_Influence_of_Lignin_Removal_on_the_Energy_Balance_of_Future_Pulp_Mills (visited on 11/26/2024).

[16] *Om cementfabriken i Slite*. sv. URL: https://www.cement.heidelbergmaterials.se/sv/slite (visited on 11/26/2024).

[17] *Heidelberg Materials CCS-projekt i Slite mot nästa fas med viktiga framsteg — Heidelberg Materials Cement Sverige*. sv. URL: https://www.cement.heidelbergmaterials.se/sv/heidelberg-materials-ccs-projekt-i-slite-mot-nasta-fas-med-viktiga-framsteg (visited on 11/26/2024).

[18] *First images — Slite CCS*. en. URL: https://www.sliteccs.se/en/first-images (visited on 11/28/2024).

[19] *World's largest ATR-based methanol plant has been put into successful operation*. en-us. URL: https://www.topsoe.com/blog/worlds-largest-atr-based-methanol-plant-has-been-put-into-successful-operation (visited on 11/27/2024).

[20] *Heidelberg Materials ansöker om 30-årigt tillstånd för brytning av kalksten för cementproduktion i Slite — Heidelberg Materials Cement Sverige*. sv. URL: https://www.cement.heidelbergmaterials.se/sv/heidelberg-materials-ansoker-om-30-arigt-tillstand-for-brytning-av-kalksten-for-cementproduktion-i-slite (visited on 11/27/2024).

[21] Talieh Rajabloo et al. "Carbon capture and utilization for industrial applications". In: *Energy Reports*. 2022 2nd International Joint Conference on Energy and Environmental Engineering 9 (Apr. 2023), pp. 111–116. ISSN: 2352-4847. DOI: 10.1016/j.egyr.2022.12.009. URL: https://www.sciencedirect.com/science/article/pii/S2352484722026087 (visited on 11/15/2024).

[22] *Figure 3. Schematic flow diagrams of post-combustion capture,...* en. URL: https://www.researchgate.net/figure/Schematic-flow-diagrams-of-post-combustion-capture-pre-combustion-capture-and-oxy-fuel_fig2_367171478 (visited on 12/05/2024).

[23] Wan Yun Hong. "A techno-economic review on carbon capture, utilisation and storage systems for achieving a net-zero CO2 emissions future". In: *Carbon Capture Science & Technology* 3 (June 2022), p. 100044. ISSN: 2772-6568. DOI: 10.1016/j.ccst.2022.100044. URL: https://www.sciencedirect.com/science/article/pii/S277265682200015X (visited on 11/15/2024).

[24] Paweł Madejski et al. "Methods and Techniques for CO2 Capture: Review of Potential Solutions and Applications in Modern Energy Technologies". en. In: *Energies* 15.3 (Jan. 2022). Code: Energies, p. 887. ISSN: 1996-1073. DOI: 10.3390/en15030887. URL: https://www.mdpi.com/1996-1073/15/3/887 (visited on 11/10/2024).

[25] K. M. S. Salvinder et al. "An overview on control strategies for CO2 capture using absorption/stripping system". In: *Chemical Engineering Research and Design* 147 (July 2019), pp. 319–337. ISSN: 0263-8762. DOI: 10.1016/j.cherd.2019.04.034. URL: https://www.sciencedirect.com/science/article/pii/S026387621930200X (visited on 11/19/2024).

[26] Tohid N.Borhani and Meihong Wang. "Role of solvents in CO2 capture processes: The review of selection and design methods". en. In: *Renewable and Sustainable Energy Reviews* 114 (Oct. 2019). Code: Renewable and Sustainable Energy Reviews, p. 109299. ISSN: 13640321. DOI: 10.1016/j.rser.2019.109299. URL: https://linkinghub.elsevier.com/retrieve/pii/S1364032119305076 (visited on 11/10/2024).

[27] Nikolai Kolev. "Chapter 1 - Basic information". In: *Packed Bed Columns*. Ed. by Nikolai Kolev. Amsterdam: Elsevier Science, Jan. 2006, pp. 1–94. ISBN: 978-0-444-52829-2. DOI: 10.1016/B978-044452829-2/50003-0. URL: https://www.sciencedirect.com/science/article/pii/B9780444528292500030 (visited on 11/11/2024).

[28] Parisa Tabarzadi and Ahad Ghaemi. "Modeling and optimization of CO2 capture in spray columns via artificial neural networks and response surface methodology". In: *Case Studies in Chemical and Environmental Engineering* 10 (Dec. 2024), p. 100783. ISSN: 2666-0164. DOI: 10.1016/j.cscee.2024.100783. URL: https://www.sciencedirect.com/science/article/pii/S2666016424001774 (visited on 11/11/2024).

[29] Oliver Seyboth et al. "Development of a Spray Scrubbing Process for Post Combustion CO2 Capture with Amine Based Solvents". In: *Energy Procedia*. 12th International Conference on Greenhouse Gas Control Technologies, GHGT-12 63 (Jan. 2014), pp. 1667–1677. ISSN: 1876-6102. DOI: 10.1016/j.egypro.2014.11.176. URL: https://www.sciencedirect.com/science/article/pii/S1876610214019912 (visited on 11/11/2024).

[30] E.J. Henley, J.D. Seader, and D.K. Roper. *Separation process principles*. Wiley, 2011. ISBN: 978-0-470-64611-3. URL: https://books.google.se/books?id=CUo8bwAACAAJ.

[31] Julien Gervasi, Lionel Dubois, and Diane Thomas. "Simulation of the Post-combustion CO2 Capture with Aspen HysysTM Software: Study of Different Configurations of an Absorption-regeneration Process for the Application to Cement Flue Gases". In: *Energy Procedia*. 12th International Conference on Greenhouse Gas Control Technologies, GHGT-12 63 (Jan. 2014), pp. 1018–1028. ISSN: 1876-6102. DOI: 10.1016/j.egypro.2014.11.109. URL: https://www.sciencedirect.com/science/article/pii/S1876610214019249 (visited on 11/11/2024).

[32] Amod Parkhi, Selen Cremaschi, and Zhihua Jiang. "Techno-Economic Analysis of CO2 Capture from Pulp and Paper Mill Limekiln". In: *IFAC-PapersOnLine*. 13th IFAC Symposium on Dynamics and Control of Process Systems, including Biosystems DYCOPS 2022 55.7 (Jan. 2022), pp. 284–291. ISSN: 2405-8963. DOI: 10.1016/j.ifacol.2022.07.458. URL: https://www.sciencedirect.com/science/article/pii/S2405896322008643 (visited on 11/11/2024).

[33] Jack Wells et al. "Simulation and modelling study of a chemical absorption plant to evaluate capture effectiveness when treating high CO2 content iron and steel industry emissions". In: *Fuel* 380 (Jan. 2025), p. 133189. ISSN: 0016-2361. DOI: 10.1016/j.fuel.2024.133189. URL: https://www.sciencedirect.com/science/article/pii/S001623612402338X (visited on 11/11/2024).

[34] Jiayi Ren et al. "Techno-economic analysis and optimisation of Piperazine-based Post-combustion carbon capture and CO2 compression process for large-scale biomass-fired power plants through simulation". In: *Fuel* 381 (Feb. 2025), p. 133340. ISSN: 0016-2361. DOI: 10.1016/j.fuel.2024.133340. URL: https://www.sciencedirect.com/science/article/pii/S001623612402489X (visited on 11/11/2024).

[35] D. James. "Failing Drop CO2 Deposition (Desublimation) Heat Exchanger for the Cryogenic Carbon Capture Process". In: 2011. URL: https://www.semanticscholar.org/paper/Failing-Drop-CO2-Deposition-(Desublimation)-Heat-James/2e1cad2b879f922cc828a398df52a5b28 (visited on 11/20/2024).

[36] A. G. Olabi et al. "Membrane-based carbon capture: Recent progress, challenges, and their role in achieving the sustainable development goals". In: *Chemosphere* 320 (Apr. 2023), p. 137996. ISSN: 0045-6535. DOI: 10.1016/j.chemosphere.2023.137996. URL: https://www.sciencedirect.com/science/article/pii/S0045653523002631 (visited on 11/20/2024).

[37] Rujing Hou et al. "Current status and advances in membrane technology for carbon capture". In: *Separation and Purification Technology* 300 (Nov. 2022), p. 121863. ISSN: 1383-5866. DOI: 10.1016/j.seppur.2022.121863. URL: https://www.sciencedirect.com/science/article/pii/S1383586622014186 (visited on 11/20/2024).

[38] Zhongde Dai and Liyuan Deng. "Membranes for CO2 capture and separation: Progress in research and development for industrial applications". In: *Separation and Purification Technology* 335 (May 2024), p. 126022. ISSN: 1383-5866. DOI: 10.1016/j.seppur.2023.126022. URL: https://www.sciencedirect.com/science/article/pii/S1383586623029301 (visited on 11/20/2024).

[39] Cristina. *Comparing Absorption and Adsorption in Carbon Capture*. en. URL: https://blog.novomof.com/comparing-absorption-and-adsorption-in-carbon-capture (visited on 11/19/2024).

[40] SGU. *Carbon capture and storage (CCS)*. en. 2020. URL: https://www.sgu.se/en/physical-planning/carbon-capture-and-storage-ccs/ (visited on 12/03/2024).

[41] IEA. "CO2 Storage Resources and their Development - An IEA CCUS Handbook". en. In: (2022).

[42] Lena Mikhelkis and Venkatesh Govindarajan. "Techno-Economic and Partial Environmental Analysis of Carbon Capture and Storage (CCS) and Carbon Capture, Utilization, and Storage (CCU/S): Case Study from Proposed Waste-Fed District-Heating Incinerator in Sweden". en. In: *Sustainability* 12.15 (Jan. 2020). Number: 15 Publisher: Multidisciplinary Digital Publishing Institute, p. 5922. ISSN: 2071-1050. DOI: 10.3390/su12155922. URL: https://www.mdpi.com/2071-1050/12/15/5922 (visited on 12/03/2024).

[43] Adrian Lefvert et al. "What are the potential paths for carbon capture and storage in Sweden? A multi-level assessment of historical and current developments". In: *Energy Research & Social Science* 87 (May 2022), p. 102452. ISSN: 2214-6296. DOI: 10.1016/j.erss.2021.102452. URL: https://www.sciencedirect.com/science/article/pii/S2214629621005399 (visited on 12/04/2024).

[44] *Northern Lights*. en-US. URL: https://norlights.com/ (visited on 11/28/2024).

[45] Gassnova. *Current Status of the Longship Project*. en. June 2024. URL: https://ccsnorway.com/current-status-of-the-longship-project/ (visited on 12/11/2024).

[46] *Project Greensand — CO2-Lagring*. en. URL: https://www.projectgreensand.com/en (visited on 12/06/2024).

[47] Youngkyun Seo et al. "Comparison of CO2 liquefaction pressures for ship-based carbon capture and storage (CCS) chain". In: *International Journal of Greenhouse Gas Control* 52 (Sept. 2016), pp. 1–12. ISSN: 1750-5836. DOI: 10.1016/j.ijggc.2016.06.011. URL: https://www.sciencedirect.com/science/article/pii/S1750583616303012 (visited on 12/02/2024).

[48] Simon Roussanaly et al. "Benchmarking of CO2 transport technologies: Part I—Onshore pipeline and shipping between two onshore areas". In: *International Journal of Greenhouse Gas Control* 19 (Nov. 2013), pp. 584–594. ISSN: 1750-5836. DOI: 10.1016/j.ijggc.2013.05.031. URL: https://www.sciencedirect.com/science/article/pii/S1750583613002478 (visited on 12/02/2024).

[49] Umer Zahid et al. "Techno-economic assessment of CO2 liquefaction for ship transportation". en. In: *Greenhouse Gases: Science and Technology* 4.6 (2014). _eprint: https://onlinelibrary.wiley.com/doi/pd pp. 734–749. ISSN: 2152-3878. DOI: 10.1002/ghg.1439. URL: https://onlinelibrary.wiley.com/doi/abs/10.1002/ghg.1439 (visited on 12/04/2024).

[50] Frithjof Engel and Alfons Kather. "Improvements on the liquefaction of a pipeline CO2 stream for ship transport". In: *International Journal of Greenhouse Gas Control* 72 (May 2018), pp. 214–221. ISSN: 1750-5836. DOI: 10.1016/j.ijggc.2018.03.010. URL: https://www.sciencedirect.com/science/article/pii/S1750583617306412 (visited on 12/03/2024).

[51] Gassnova and Gassco. *Feasibility study for full-scale CCS in Norway*. Tech. rep. 2016. URL: https://ccsnorway.com/app/uploads/sites/6/2019/09/feasibilitystudy_fullscale_ccs_norway_2016.pdf (visited on 12/02/2024).

[52] Abdullah Alabdulkarem, Yunho Hwang, and Reinhard Radermacher. "Development of CO2 liquefaction cycles for CO2 sequestration". In: *Applied Thermal Engineering* 33-34 (Feb. 2012), pp. 144–156. ISSN: 1359-4311. DOI: 10.1016/j.applthermaleng.2011.09.027. URL: https://www.sciencedirect.com/science/article/pii/S1359431111005114 (visited on 12/03/2024).

[53] Han Deng, Simon Roussanaly, and Geir Skaugen. "Techno-economic analyses of CO2 liquefaction: Impact of product pressure and impurities". In: *International Journal of Refrigeration* 103 (July 2019), pp. 301–315. ISSN: 0140-7007. DOI: 10.1016/j.ijrefrig.2019.04.011. URL: https://www.sciencedirect.com/science/article/pii/S0140700719301677 (visited on 12/03/2024).

[54] Simon Roussanaly, Amy L. Brunsvold, and Erik S. Hognes. "Benchmarking of CO2 transport technologies: Part II – Offshore pipeline and shipping to an offshore site". In: *International Journal of Greenhouse Gas Control* 28 (Sept. 2014), pp. 283–299. ISSN: 1750-5836. DOI: 10.1016/j.ijggc.2014.06.019. URL: https://www.sciencedirect.com/science/article/pii/S1750583614001765 (visited on 11/28/2024).

[55] Hope McLaughlin et al. "Carbon capture utilization and storage in review: Sociotechnical implications for a carbon reliant world". en. In: *Renewable and Sustainable Energy Reviews* 177 (May 2023), p. 113215. ISSN: 13640321. DOI: 10.1016/j.rser.2023.113215. URL: https://linkinghub.elsevier.com/retrieve/pii/S1364032123000710 (visited on 12/06/2024).

[56] Shadfar Davoodi et al. "Carbon dioxide sequestration through enhanced oil recovery: A review of storage mechanisms and technological applications". In: *Fuel* 366 (June 2024), p. 131313. ISSN: 0016-2361. DOI: 10.1016/j.fuel.2024.131313. URL: https://www.sciencedirect.com/science/article/pii/S0016236124004605 (visited on 12/02/2024).

[57] Seungwoo Kang et al. *Innovation outlook: renewable methanol*. eng. Ed. by Dolf Gielen and Greg Dolan. Abu Dhabi: International Renewable Energy Agency, 2021. ISBN: 978-92-9260-320-5.

[58] Vanessa Núñez-López and Emily Moskal. "Potential of CO2-EOR for Near-Term Decarbonization". In: *Frontiers in Climate* 1 (Sept. 2019), p. 5. ISSN: 2624-9553. DOI: 10.3389/fclim.2019.00005. URL: https://www.frontiersin.org/article/10.3389/fclim.2019.00005/full (visited on 12/09/2024).

[59] T.A. Meckel et al. "Carbon capture, utilization, and storage hub development on the Gulf Coast". en. In: *Greenhouse Gases: Science and Technology* 11.4 (Aug. 2021), pp. 619–632. ISSN: 2152-3878, 2152-3878. DOI: 10.1002/ghg.2082. URL: https://onlinelibrary.wiley.com/doi/10.1002/ghg.2082 (visited on 12/09/2024).

[60] Patrizio Battaglia et al. "Methanol synthesis through CO2 capture and hydrogenation: Thermal integration, energy performance and techno-economic assessment". en. In: *Journal of CO2 Utilization* 44 (Feb. 2021). Code: Journal of CO2 Utilization, p. 101407. ISSN: 22129820. DOI: 10.1016/j.jcou.2020.101407. URL: https://linkinghub.elsevier.com/retrieve/pii/S2212982020310374 (visited on 11/06/2024).

[61] Renata Vardanega et al. "Supercritical fluid processing and extraction of food". en. In: *Green Food Processing Techniques*. Elsevier, 2019, pp. 57–86. ISBN: 978-0-12-815353-6. DOI: 10.1016/B978-0-12-815353-6.00003-3. URL: https://linkinghub.elsevier.com/retrieve/pii/B9780128153536000033 (visited on 12/09/2024).

[62] Can Erkey. "Supercritical carbon dioxide extraction of metals from aqueous solutions: a review". en. In: *The Journal of Supercritical Fluids* 17.3 (June 2000), pp. 259–287. ISSN: 08968446. DOI: 10.1016/S0896-8446(99)00047-9. URL: https://linkinghub.elsevier.com/retrieve/pii/S0896844699000479 (visited on 12/09/2024).

[63] Daniel A. Bertuol et al. "Recovery of cobalt from spent lithium-ion batteries using supercritical carbon dioxide extraction". en. In: *Waste Management* 51 (May 2016), pp. 245–251. ISSN: 0956053X. DOI: 10.1016/j.wasman.2016.03.009. URL: https://linkinghub.elsevier.com/retrieve/pii/S0956053X16300964 (visited on 12/09/2024).

[64] Christof Kersch et al. "Municipal waste incinerator fly ash: supercritical fluid extraction of metals". en. In: *Journal of Chemical Technology & Biotechnology* 77.3 (Mar. 2002), pp. 256–259. ISSN: 0268-2575, 1097-4660. DOI: 10.1002/jctb.589. URL: https://onlinelibrary.wiley.com/doi/10.1002/jctb.589 (visited on 12/09/2024).

[65] Guanrong Song et al. "Extraction of selected rare earth elements from anthracite acid mine drainage using supercritical CO2 via coagulation and complexation". en. In: *Journal of Rare Earths* 39.1 (Jan. 2021), pp. 83–89. ISSN: 10020721. DOI: 10.1016/j.jre.2020.02.007. URL: https://linkinghub.elsevier.com/retrieve/pii/S1002072119307744 (visited on 12/09/2024).

[66] Michael Bowker. "Methanol Synthesis from CO_2 Hydrogenation". en. In: *ChemCatChem* 11.17 (Sept. 2019), pp. 4238–4246. ISSN: 1867-3880, 1867-3899. DOI: 10.1002/cctc.201900401. URL: https://chemistry-europe.onlinelibrary.wiley.com/doi/10.1002/cctc.201900401 (visited on 12/05/2024).

[67] G.H. Graaf, E.J. Stamhuis, and A.A.C.M. Beenackers. "Kinetics of low-pressure methanol synthesis". en. In: *Chemical Engineering Science* 43.12 (1988). Code: Chemical Engineering Science, pp. 3185–3195. ISSN: 00092509. DOI: 10.1016/0009-2509(88)85127-3. URL: https://linkinghub.elsevier.com/retrieve/pii/0009250988851273 (visited on 11/06/2024).

[68] Éverton Simões Van-Dal and Chakib Bouallou. "Design and simulation of a methanol production plant from CO2 hydrogenation". en. In: *Journal of Cleaner Production* 57 (Oct. 2013). Code: Journal of Cleaner Production, pp. 38–45. ISSN: 09596526. DOI: 10.1016/j.jclepro.2013.06.008. URL: https://linkinghub.elsevier.com/retrieve/pii/S0959652613003892 (visited on 11/06/2024).

[69] Noor Yusuf and Fares Almomani. "Highly effective hydrogenation of CO2 to methanol over Cu/ZnO/Al2O3 catalyst: A process economy & environmental aspects". en. In: *Fuel* 332 (Jan. 2023). Code: Fuel, p. 126027. ISSN: 00162361. DOI: 10.1016/j.fuel.2022.126027. URL: https://linkinghub.elsevier.com/retrieve/pii/S0016236122028514 (visited on 11/06/2024).

[70] Judit Nyári et al. "Choice of the kinetic model significantly affects the outcome of techno-economic assessments of CO2-based methanol synthesis". en. In: *Energy Conversion and Management* 271 (Nov. 2022), p. 116200. ISSN: 01968904. DOI: 10.1016/j.enconman.2022.116200. URL: https://linkinghub.elsevier.com/retrieve/pii/S0196890422009773 (visited on 11/20/2024).

[71] Esteban L. Fornero et al. "CO2 capture via catalytic hydrogenation to methanol: Thermodynamic limit vs. 'kinetic limit'". en. In: *Catalysis Today* 172.1 (Aug. 2011). Code: Catalysis Today, pp. 158–165. ISSN: 09205861. DOI: 10.1016/j.cattod.2011.02.036. URL: https://linkinghub.elsevier.com/retrieve/pii/S0920586111001520 (visited on 11/11/2024).

[72] *IMPCA METHANOL REFERENCE SPECIFICATIONS*. June 2021.

[73] Nan Wang et al. "MEA-based CO2 capture: a study focuses on MEA concentrations and process parameters". English. In: *Frontiers in Energy Research* 11 (Sept. 2023). Publisher: Frontiers. ISSN: 2296-598X. DOI: 10.3389/fenrg.2023.1230743. URL: https://www.frontiersin.org/journals/energy-research/articles/10.3389/fenrg.2023.1230743/full (visited on 12/04/2024).

[74] Li B.H., Zhang N., and Smith R. "Rate-based modelling of co2 capture process by reactive absorption with mea". en. In: *Chemical Engineering Transactions* 39 (Aug. 2014), pp. 13–18. DOI: 10.3303/CET1439003. URL: https://doi.org/10.3303/CET1439003 (visited on 12/04/2024).

[75] *Lag (1990:613) om miljöavgift på utsläpp av kväveoxider vid energiproduktion*. sv. URL: https://www.riksdagen.se/sv/dokument-och-lagar/dokument/svensk-forfattningssamling/lag-1990613-om-miljoavgift-pa-utslapp-av_sfs-1990-613/ (visited on 12/06/2024).

[76] "Rate-Based Model of the CO2 Capture Process by MEA using Aspen Plus". en. In: ().

[77] Youngkyun Seo et al. "Evaluation of CO2 liquefaction processes for ship-based carbon capture and storage (CCS) in terms of life cycle cost (LCC) considering availability". In: *International Journal of Greenhouse Gas Control* 35 (Apr. 2015), pp. 1–12. ISSN: 1750-5836. DOI: 10.1016/j.ijggc.2015.01.006. URL: https://www.sciencedirect.com/science/article/pii/S1750583615000134 (visited on 11/28/2024).

[78] Maurice Stewart. "7 - Compressor fundamentals". In: *Surface Production Operations*. Ed. by Maurice Stewart. Boston: Gulf Professional Publishing, Jan. 2019, pp. 457–525. ISBN: 978-0-12-809895-0. DOI: 10.1016/B978-0-12-809895-0.00007-7. URL: https://www.sciencedirect.com/science/article/pii/B9780128098950000077 (visited on 11/28/2024).

[79] *Google Earth*. URL: https://earth.google.com/web/@0,-2.31930005,0a,22251752.77375655d,35y,0h,0t,0r/data=CgRCAggBOgMKATBCAggBSg0I__________ARAA (visited on 12/05/2024).

[80] Youngkyun Seo et al. "Determination of optimal volume of temporary storage tanks in a ship-based carbon capture and storage (CCS) chain using life cycle cost (LCC) including unavailability cost". In: *International Journal of Greenhouse Gas Control* 64 (Sept. 2017), pp. 11–22. ISSN: 1750-5836. DOI: 10.1016/j.ijggc.2017.06.017. URL: https://www.sciencedirect.com/science/article/pii/S1750583616304182 (visited on 12/09/2024).

[81] K.M. Vanden Bussche and G.F. Froment. "A Steady-State Kinetic Model for Methanol Synthesis and the Water Gas Shift Reaction on a Commercial Cu/ZnO/Al2O3Catalyst". en. In: *Journal of Catalysis* 161.1 (June 1996), pp. 1–10. ISSN: 00219517. DOI: 10.1006/jcat.1996.0156. URL: https://linkinghub.elsevier.com/retrieve/pii/S0021951796901566 (visited on 12/11/2024).

[82] *Fluid Mechanics*. URL: https://www.training.itservices.manchester.ac.uk/public/gced/CEPCI.html?reactors/CEPCI/index.html (visited on 12/05/2024).

[83] *Startsida*. sv. URL: https://www.riksbank.se/sv/ (visited on 12/09/2024).

[84] R. K. Sinnott and Gavin P. Towler. *Chemical engineering design*. eng. 6th edition. Coulson & Richardson's Chemical engineering series. Oxford: Elsevier, 2020. ISBN: 978-0-08-102599-4.

[85] M. M. Jaffar et al. "Comparative techno-economic analysis of the integration of MEA-based scrubbing and silica PEI adsorbent-based CO2 capture processes into cement plants". In: *Journal of Cleaner Production* 414 (Aug. 2023), p. 137666. ISSN: 0959-6526. DOI: 10.1016/j.jclepro.2023.137666. URL: https://www.sciencedirect.com/science/article/pii/S0959652623018243 (visited on 12/12/2024).

[86] Jaesung Kum et al. "Techno-economic analysis and optimization of a CO2 absorption process with a solvent looping system at the absorber using an MDEA/PZ blended solvent for steam methane reforming". In: *Chemical Engineering Journal* 455 (Jan. 2023), p. 140685. ISSN: 1385-8947. DOI: 10.1016/j.cej.2022.140685. URL: https://www.sciencedirect.com/science/article/pii/S1385894722061654 (visited on 12/09/2024).

[87] "European Hydrogen Observatory". *Cost of hydrogen production*. 2023. URL: https://observatory.clean-hydrogen.europa.eu/index.php/hydrogen-landscape/production-trade-and-cost/cost-hydrogen-production (visited on 12/06/2024).

[88] *Monoethanolamine price trend and forecast - Raw chemical materials supplier and manufacturer*. en-GB. Section: article. Aug. 2024. URL: https://archemco.com/2024/08/04/monoethanolamine-price-trend-and-forecast/ (visited on 12/09/2024).

[89] Alex Schmitt. *EU Energy Outlook 2050: How will the European electricity market develop over the next 30 years?* en-US. Apr. 2022. URL: https://blog.energybrainpool.com/en/eu-energy-outlook-2050-how-will-the-european-electricity-market-develop-over-the-next-30-years/ (visited on 12/09/2024).

[90] Mehdi Karimi, Magne Hillestad, and Hallvard F. Svendsen. "Capital costs and energy considerations of different alternative stripper configurations for post combustion CO2 capture". en. In: *Chemical Engineering Research and Design* 89.8 (Aug. 2011), pp. 1229–1236. ISSN: 02638762. DOI: 10.1016/j.cherd.2011.03.005. URL: https://linkinghub.elsevier.com/retrieve/pii/S0263876211001122 (visited on 12/09/2024).

[91] Sarath C. Gowd et al. "Economic perspectives and policy insights on carbon capture, storage, and utilization for sustainable development". en. In: *Science of The Total Environment* 883 (July 2023), p. 163656. ISSN: 00489697. DOI: 10.1016/j.scitotenv.2023.163656. URL: https://linkinghub.elsevier.com/retrieve/pii/S0048969723022763 (visited on 12/05/2024).

[92] Regeringen och Regeringskansliet. *Sweden's carbon tax*. en. Text. Publisher: Regeringen och Regeringskansliet. Feb. 2018. URL: https://www.government.se/government-policy/taxes-and-tariffs/swedens-carbon-tax/ (visited on 12/05/2024).

[93] *What is the EU ETS? - European Commission*. en. URL: https://climate.ec.europa.eu/eu-action/eu-emissions-trading-system-eu-ets/what-eu-ets_en (visited on 12/05/2024).

[94] *Emissions Trading and Carbon Capture and Storage: Mapping possible interactions, technical considerations, and existing provisions — International Carbon Action Partnership*. en. Feb. 2023. URL: https://icapcarbonaction.com/en/publications/emissions-trading-and-carbon-capture-and-storage-mapping-possible-interactions (visited on 12/09/2024).

[95] Kristin Onarheim et al. "Performance and cost of CCS in the pulp and paper industry part 2: Economic feasibility of amine-based post-combustion CO 2 capture". en. In: *International Journal of Greenhouse Gas Control* 66 (Nov. 2017), pp. 60–75. ISSN: 17505836. DOI: 10.1016/j.ijggc.2017.09.010. URL: https://linkinghub.elsevier.com/retrieve/pii/S1750583617303766 (visited on 12/09/2024).

[96] *EU Carbon Permits - Price - Chart - Historical Data - News*. URL: https://tradingeconomics.com/commodity/carbon (visited on 12/08/2024).

[97] *Forecast EU-ETS carbon prices 2024-2035*. en. URL: https://www.statista.com/statistics/1401657/forecast-average-carbon-price-eu-emissions-trading-system/ (visited on 12/09/2024).

[98] *Methanol - Price - Chart - Historical Data - News*. URL: https://tradingeconomics.com/commodity/methanol (visited on 12/08/2024).

[99] *Methanol Market Size, Share & Growth Analysis Report 2030*. en. URL: https://www.grandviewresearch.com/industry-analysis/methanol-market (visited on 12/09/2024).

[100] Dirk Schoenmaker and Willem Schramade. "Which discount rate for sustainability?" In: *Journal of Sustainable Finance and Accounting* 3 (Sept. 2024), p. 100010. ISSN: 2950-3701. DOI: 10.1016/j.josfa.2024.100010. URL: https://www.sciencedirect.com/science/article/pii/S2950370124000105 (visited on 12/06/2024).

[101] Bert Metz and Intergovernmental Panel on Climate Change, eds. *IPCC special report on carbon dioxide capture and storage*. eng. 1. publ. Cambridge: Cambridge Univ. Press, 2005. ISBN: 978-0-521-86643-9 978-0-521-68551-1.